Friday 10th January, 2025

Ecole Polytechnique Fédérale de Lausanne

Urban Thermodynamics

Group Project

Groupe 5:
Aurélien Sapin
Yvan Bruno
Lilia Perraudin
Lara Freitas Florencio
Carla Regenass

Professor: Dolaana Khovalyg
Teaching Assistant: Kun Lyu

Table of contents

1 Introduction

The rapid growth of urban areas has created significant environmental challenges, especially urban overheating, which affects human comfort, health, and energy needs. This project examines how different urban elements influence the microclimate and energy exchanges within EPFL Innovation Park in Ecublens, Switzerland, near the city of Lausanne. By studying site-specific features and testing potential interventions, we aim to find effective strategies to reduce urban overheating and strengthen the park's thermal resilience.

Our approach has three main phases: (1) assessing the site's characteristics and current thermal conditions, (2) analyzing how buildings, vegetation, water bodies, and ground surfaces affect the local microclimate, and (3) exploring the combination of targeted interventions to enhance human comfort and energy efficiency. Using ENVI-met microclimate simulations and climate data for 2021, we will study how these elements interact under the given conditions to help us select the most effective urban design solutions.

2 Site Analysis

The EPFL Innovation Park consists of a dynamic and organized layout designed to accommodate research, innovation, and collaborative spaces within a green and structured environment.

2.1 Climate analysis

The EPFL Innovation Park has an area of approximately 11 hectares and is located in the southwestern part of the EPFL campus near Lake Geneva. Its local climatic conditions is influenced by its surrounding, including temperature regulation from the lake and potential urban heat island (UHI) effects from infrastructures. The site is bordered by roads on three sides and residential areas to its west and south. These roads are localized anthropogenic heat sources.

The Innovation Park area experiences warm summers, with temperatures reaching until 38°C. In winter, temperatures can drop below 0°C. The relative humidity has an average of 70% in summer, which is less humid then winter, with values around 80%. Due to the low angle of the Sun, shortwave radiation is significantly low (around 100 W/m^2) in winter, meanwhile the longwave radiation is about 400 [W/m^2]. In summer, the shortwave radiation is much higher with values peaking above 600 [W/m^2], while longwave are slightly higher than in winter, due to warmer surfaces. The area is also subject to cold north-eastern winds, particularly in winter, which therefore do not contribute to cooling during the summer months. These wind patterns are critical to consider for optimizing building orientation, implementing windbreaks, and enhancing natural ventilation in urban planning.

2.2 Urban layout and materials

The site features a cluster of rectilinear office buildings and is structured around a central open space (Figure 2). These clusters are separated by pathways, greenery, and open spaces for circulation and interaction. The buildings are grouped into three main types:

- Orange Buildings (group A): Represent square-shaped, compact buildings distributed across the central area.
- Blue Buildings (group B): Represent elongated rectangular structures located primarily on the northern side of the site.
- Purple Building (group C): A single compact rectangular structure located on the northeast side of the site.

Around the buildings, there are roads made of asphalt with a high heat absorption capacity and low albedo. This results in an increased UHI effect especially during summer months. The pathways are mostly

made of sandy soil and gravel, allowing more water absorption. On one side of the site, an urban woodland provides some shade which reduces surface temperatures and enhances evapotranspiration. On the other side, there is a parking lot. It is mostly made of asphalt and partially of gravel. Therefore, the parking lot has a low albedo, can absorb a significant amount of radiation, and retains heat effectively. Additionally, it is a source of anthropogenic heat. Therefore in one of the modifications, the parking lot was replaced by a green area, supposing that an underground parking can be realized.

The building facade and roof composition are described in Figure 48 in Annex. For modeling the EPFL Innovation Park in ENVI-met it is necessary to obtain some of the thermal properties of the materials, see Table 1 in Annex.

The external layer (Layer 1 in the description) is the most critical in determining how a building interacts with its environment. The external layers of the building facades and roofs in the site typically exhibit moderate to high absorption values (0.6 to 0.8), except Group C's facade, which has a lower absorption value of 0.5. These materials also have moderate to high density, which, together with their absorption properties, allows for significant heat storage and delayed heat release. This combination intensifies the urban heat island (UHI) effect by increasing surface temperatures and prolonging nighttime heat dissipation.

It is worth noting that the only building on the site of type C performs better than the others. Its facade has a lower combined thickness, which reduces the material's heat storage potential. Additionally, the materials are more reflective, helping to mitigate the urban heat island (UHI) effect, and have lower thermal conductivity and density, decreasing heat transfer and improving energy efficiency. This combination results in a lighter negative impact on the environment.

2.3 Urban morphology

The Innovation Park is classified as an open mid-rise area (LCZ 5) within the Local Climate Zone (LCZ) framework, characterized by wide green spaces between buildings. A picture of the site can be found in the Annex (Figure 50). The LCZ classification aids in assessing factors such as impermeability, surface roughness, thermal behavior, and energy and water usage.

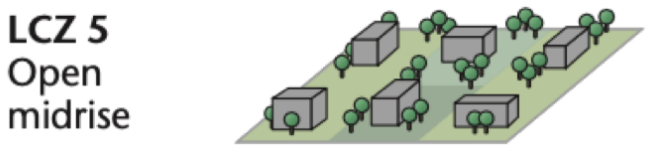

Figure 1: LCZ categorization

The Sky View Factor (SVF) in urban areas quantifies the portion of the sky visible from a particular point, which affects microclimate elements like solar radiation, heat retention, and cooling rates. On the site, the sky view factor (SVF) varies between 0.4 and 0.9 (Figure put figure in the annex). The majority of the area exhibits an SVF ranging from 0.5 to 0.8. The lowest sky view factor can be observed between the buildings of group A, which are the most closely spaced. These buildings also exhibit the highest canyon aspect ratio. Conversely, the highest SVF values are found where the buildings are spaced furthest apart. The urban woodland features an SVF ranging between 0.8 and 0.9 but this results from an approximation in ENVIMET where the forest consists of nine trees.

In open mid-rise urban areas, the SVF typically ranges between 0.4 and 0.6. This range reflects a moderate degree of openness, where mid-rise buildings allow some sky visibility but also produce shading and reduced sky exposure.

The heights of the buildings range from 13m to 22m. The distances between the buildings vary significantly, as well as the canyon aspect ratio. It is ranging between 0.36 and 1.5.

The canyon aspect ratio can be calculated by taking the average height of the two buildings and dividing it by the distance between them. The canyon aspect ratio influences the urban heat island (UHI) effect, among other factors. The maximum night UHI intensity can be calculated using the following formula:

$$\mathrm{UHI}_{\mathrm{mag}} = 7.54 + 3.97 \cdot \ln\left(\frac{H}{W}\right) \tag{1}$$

In the case of the analyzed buildings, the maximum night UHI intensity varies between 3.6°C and 9.14°C. In the case of the study site, however, the buildings are very scattered, so the canyon aspect ratio is not very relevant, as there are no true urban canyons. The scattered arrangement of the buildings influences the wind profile. The scattered formation helps to prevent wind bursts but allows for air mixing.

2.4 Green elements

Most of the green areas are fully covered with trees. Each building is surrounded by a small lane of vegetation. Therefore, vegetation is well distributed all over the area. The parking lot is lined with trees as well. Small areas of grass are present in the center of the park.

In the following analysis, 12 00 was chosen as the reference time. At this hour, the sun is close to its highest point and the latent heat flux is often maximal. Additionally, many people are typically outdoors at this time as their lunch breaks begins. They are affected by the Urban Heat Island (UHI) effect and would benefit from measures to mitigate it.

3 Base Case: simulations results analysis

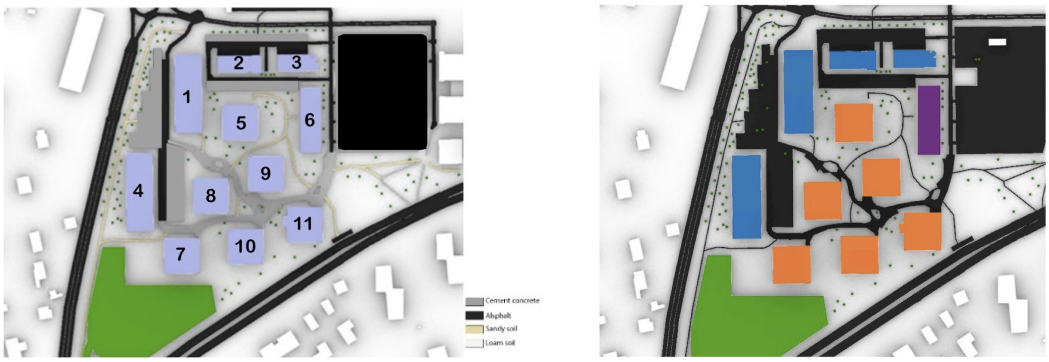

Figure 2: Base case model description of EPFL Innovation Park

The microclimatic dynamics of the Innovation Park are influenced by a range of interacting factors, as outlined earlier. To evaluate the site's thermal performance, ENVI-met simulations were analyzed, focusing on air temperature, relative humidity, surface temperature, wind patterns, and radiation. All key parameters for understanding baseline conditions and identifying areas for improvement.

August 18, 2021, was selected as a reference, representing one of the hottest days in the dataset to evaluate extreme weather conditions. Midday simulations, reflecting peak occupancy hours when people are most exposed to thermal discomfort, were prioritized for assessing mitigation strategies. These noon results provide a robust basis for addressing the Urban Heat Island (UHI) effect.

For the base case, a midnight analysis (in Annex A.1) was included to understand nighttime heat dissipation and its influence on daytime conditions. This complementary analysis offers broader insights into the

site's thermal behavior, supporting the development of targeted interventions.

3.1 Potential air temperature

Potential air temperature is a standardized metric that adjusts temperature measurements to a reference pressure level, typically at sea level. This parameter facilitates a more precise analysis of thermal dynamics by isolating the effects of heating, cooling, and atmospheric processes from variations caused by altitude or pressure changes.

At midday, the air temperature ranges from a minimum of 36.47°C to a maximum of 40.65°C. The simulation highlights several thermal hotspots, notably the parking lot in the upper-right corner and the two main roads, both being surfaces of asphalt. In contrast, cooler areas are observed around the square buildings, likely due to their greater height, which increases the shading they provide to surrounding areas.

Additionally, cooler zones are detected behind Buildings 1, 2, and 3, while warmer zones are present in front of these structures. By comparing temperature patterns with the distribution of ground materials, shading emerges as the most significant factor influencing air temperature. This hypothesis will be further verified by analyzing surface temperature and radiation patterns to confirm the role of shading in mitigating heat.

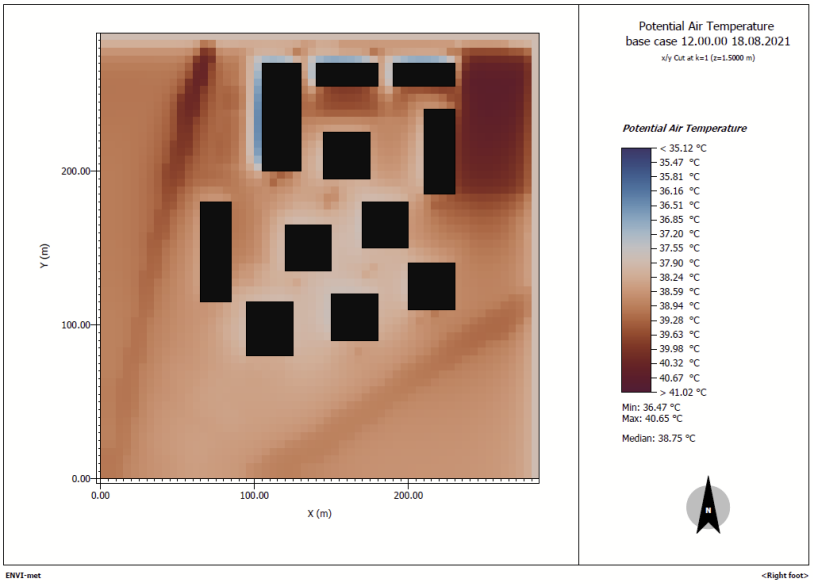

Figure 3: Potential air temperature diagram for the base case at midday

3.2 Surface temperature

At midday, surface temperatures range from 19.85°C to 49.15°C, highlighting a big difference between the various surface present on the site. The coolest surfaces are located around the buildings, particularly along the north and west facades. This consistent pattern across all buildings suggests that shading is the primary factor, as corroborated by the shortwave radiation diagram. Notably, these shaded zones are slightly larger around the taller square buildings, which stand at 22 meters, providing more extensive shading. It is also noticed small variations of surface temperatures within the shaded areas.

As expected, asphalt and dark concrete surfaces emerge as thermal hotspots. With their high absorptivity and low reflectivity, these materials efficiently absorb direct solar radiation, the dominant heat source during the day. We also observe that the light concrete surfaces have a slighted lower surface temperatures than the surroundings, the higher albedo value can be used as justification since it implies that a bigger

portion of the radiation is reflected.

Interestingly, the tree canopy in the bottom-left corner exhibits moderate surface temperatures, approximately 33°C. Although the tree receives direct solar radiation similar to asphalt and concrete, part of the absorbed energy is used for physiological processes like photosynthesis and transpiration, reducing the heat retained on its surface. It is important to note that, due to capacity limitations, the tree canopy is represented by a limited number of trees, which may affect the accuracy of surface temperature values and other parameters presented in this report.

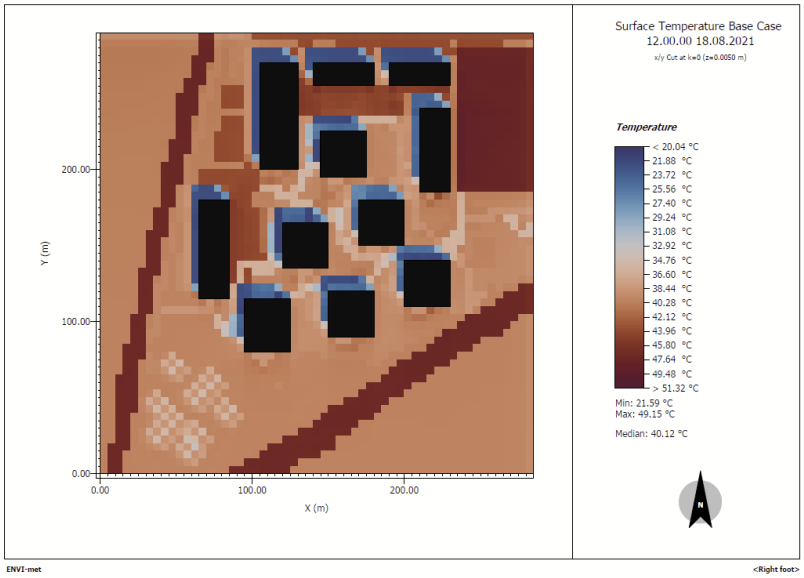

Figure 4: Surface temperature diagram for the base case at midday

3.3 Wind

At midday, the wind flow is predominantly directed from north to south, with a slight clockwise deviation. Wind speeds range from 0.01 m/s to 0.29 m/s. As expected, the wind deflects around the buildings, creating stagnation zones at the northeast and southwest corners and areas of higher wind speed at the northwest and southeast corners due to flow acceleration around the structures.

The building layout induces a diagonal trend of wind stagnation from the northeast to the southwest within the cluster, significantly reducing wind speed and restricting airflow in the central portion of the site. This results in poor air circulation and limited ventilation, which exacerbates thermal discomfort in the area.

The wind conditions in the central cluster would likely be significantly worse without the two wind corridors created by the urban canyons between buildings 1, 2, and 3. These corridors channel airflow effectively by leveraging the aerodynamic acceleration of wind through confined spaces, thereby reducing stagnation zones and enhancing localized ventilation. This effect plays a critical role in partially mitigating the otherwise poor air circulation within the cluster.

In contrast, vegetated zones and open urban areas, such as the parking lot, exhibit higher wind speeds (around 0.12 m/s). However, these speeds remain insufficient to promote adequate air renewal and cooling through mixing. The low airflow in these zones restricts the dissipation of heat and contributes to the persistence of elevated air and surface temperatures across the site.

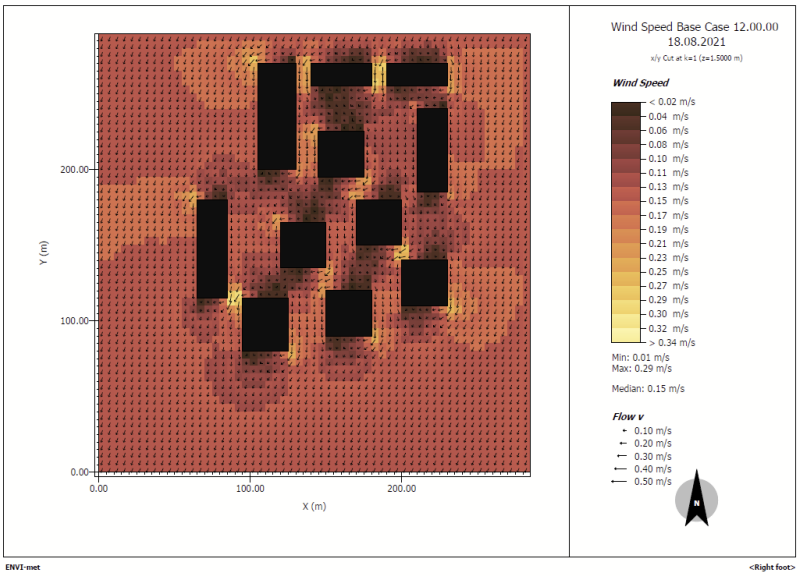

Figure 5: Wind diagram for the base case at midday

It is worth noting that the vegetation, particularly the trees in the bottom-left corner, does not appear to significantly influence wind patterns.

3.4 Relative humidity

The simulation results indicate that Relative Humidity (RH) ranges from 46.61% to 60.32%. Low RH values are consistently observed in asphalt and concrete areas, except for shaded zones behind Buildings 1, 2, and 3. This exception can be attributed to the shading effect, which reduces evaporation and allows these areas to retain more moisture, even on impermeable surfaces like asphalt. In general, the low RH in asphalt and concrete zones is due to their impermeability, which prevents water retention and causes rapid evaporation under direct sunlight.

In contrast, high RH values are found in vegetated areas, such as zones with trees and green spaces. Vegetation promotes localized cooling and increased RH through processes like photosynthesis and evapotranspiration, which regulate moisture and temperature.

Building clusters, especially taller structures like Buildings 7, 10, and 11, also contribute to higher RH values by creating shaded zones that limit evaporation. Additionally, the scattered layout of the site disrupts large-scale RH uniformity, resulting in localized moisture-retaining pockets.

This RH distribution has implications for thermal comfort. Low RH values in exposed areas can exacerbate heat stress and discomfort, while shaded and vegetated zones provide relief by maintaining higher RH and cooler conditions.

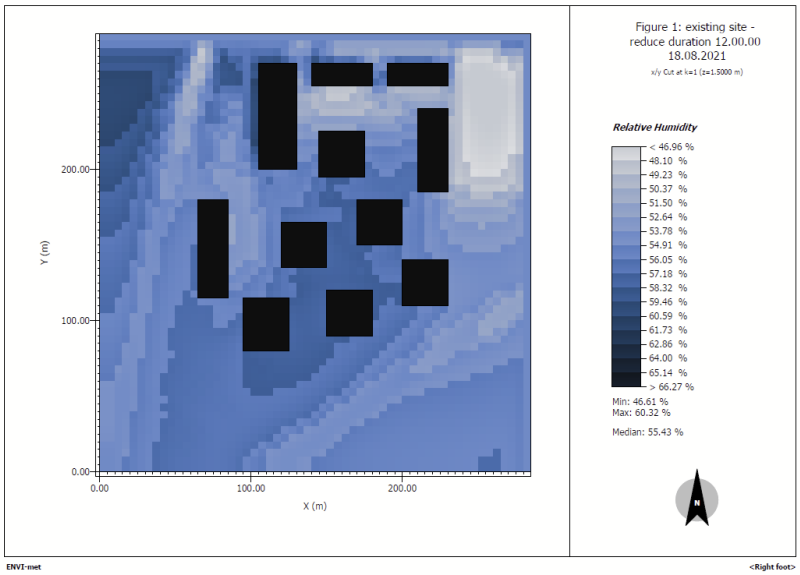

Figure 6: Relative humidity diagram for the base case at midday

3.5 Radiation

As shown in Figure 7, the reflected direct shortwave (SW) radiation distribution closely follows the distribution of ground materials (Figure 51 in Annex). The radiation values range significantly, from 20.82 W/m^2 to 407.07 W/m^2.

Low radiation zones are primarily associated with shaded areas and materials with low albedo. The shaded zones, marked in dark blue, are located along the north and west facades of the building. While areas with low albedo, such as asphalt roads, asphalt parking lots (asphalt's albedo = 0.12), and tree canopies, appear in lighter blue.

This highlights the importance of building arrangement and height in reducing SW radiation exposure. Taller structures and strategically placed buildings cast shadows that lower radiation levels in their surroundings, potentially reducing local surface and air temperatures.

In contrast, zones with particularly high reflected radiation (oscillating between yellow and red) are associated with light concrete pavement pathways, which have a particularly high albedo value of 0.5 compared to other ground materials (e.g., asphalt with albedo = 0.12, sandy loam albedo = 0.2).

Interestingly, sandy pathways, despite their low albedo of 0.0, fall within the moderate radiation range (marked in green on the diagram). This may be due to reflected radiation from nearby building facades and adjacent soil. However, the sandy pathways do exhibit slightly lower values compared to neighboring zones.

Additionally, areas within urban canyons show slightly higher radiation values (darker shades of green) compared to open spaces. However, this effect is less pronounced than the influence of ground materials, trees, or shading.

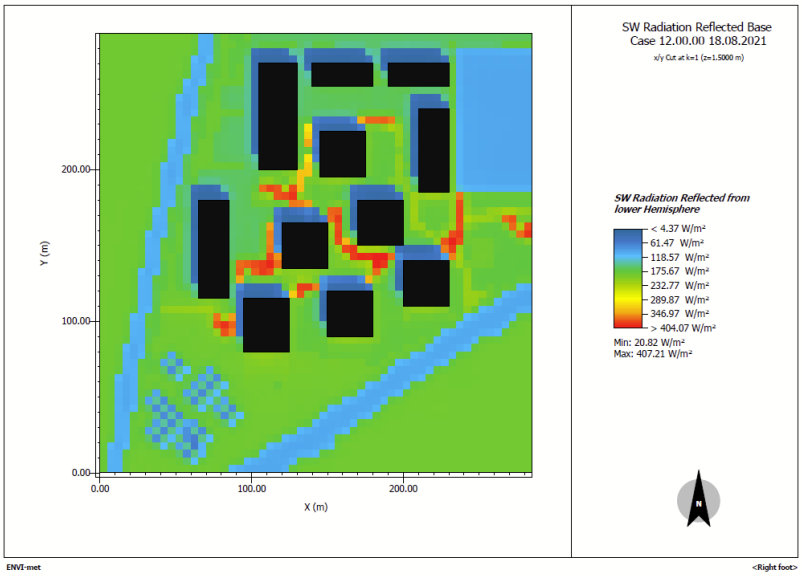

Figure 7: Reflected Shortwave radiation diagram for the base case at midday

4 Building - Environment Interaction analysis

Figures 2 and 48 illustrate the initial building configurations. Based on hotspots identified in the base case simulation, several modifications were implemented to evaluate potential mitigation strategies. These changes are detailed in Annex A.2, with a 3D representation provided in Figure 8.

In general, the modifications included the addition of a 25 cm green roof (grass) to all buildings and the greening of at least two facades per building, using either ivy or fumbia or both. Ivy was chosen for its adaptability and low maintenance requirements, while fumbia, despite its higher maintenance needs, was selected for shaded areas and low heights as it does not thrive in direct sunlight.

The materials of Buildings 5 and 8 were changed from Material B to Material C (as classified in Figure 48). Additionally, building heights were adjusted, with some structures increased and others decreased. Finally, openings were added to all buildings, alternating between or incorporating both north-south and east-west orientations.

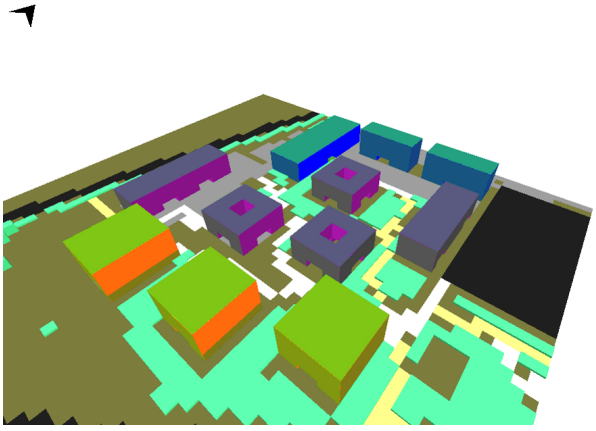

Figure 8: 3D-view of building modifications

We designed these modifications to tackle the issues previously discussed, such as thermal hotspots, restricted airflow, and inefficient building materials. For instance, adding green roofs is intended to reduce rooftop heat absorption and stabilize building temperatures, while ivy walls on the south and west facades

should help block solar radiation and provide natural cooling. Similarly, the use of fumbia walls combined with ivy on the eastern facades is expected to enhance thermal performance by mitigating heat buildup on surfaces exposed to intense morning sunlight.

Nice work of referencing to actual project and literature.

This greening strategy was inspired by buildings in Singapore, where greenery is not only used to promote cooling and mitigate the UHI effect but is also integrated into the architectural design of the city. An iconic example is the Parkroyal Collection Pickering Hotel, where the designed green space exceeds the original land area on which the hotel was built [Reference (3)]. Furthermore, research indicates that urban greening is among the most effective solutions for reducing urban warming [Reference (4)].

Inspired by another cooling strategy implemented in Singapore, the openings added to the buildings aim to increase porosity. This approach has been shown to improve the pedestrian level wind environment and cool surrounding areas. For instance, a decrease in wind speed from 1 m/s to 0.3 m/s would result in an increase of 1.9^{o}C in temperature [Reference (5)].

Building height adjustments were planned to improve shading, with taller structures strategically positioned to cast shadows on high-temperature zones, and the centralized openings on facades were introduced to facilitate better airflow and break up stagnation zones. Together, these interventions represent a hypothesis that combines shading, cooling, and ventilation strategies to improve the site's overall thermal performance. Next, we will validate this by testing those modifications through an ENVI-met simulation to analyze their impact on the urban microclimate at midday.

4.1 Potential air temperature

We begin by analyzing the simulation results (Figure 9(a)) to examine the impact of the openings, which are noticeably cooler compared to the buildings' surroundings. This aligns with the intended objective of creating thermally comfortable zones by enhancing shade and ventilation, resulting in lower temperatures.

Figure 9(b) presents a comparison of the modified building simulations against the base case ($Buildings - Base$). Negative values indicate that the mitigation strategies were effective in reducing temperatures.

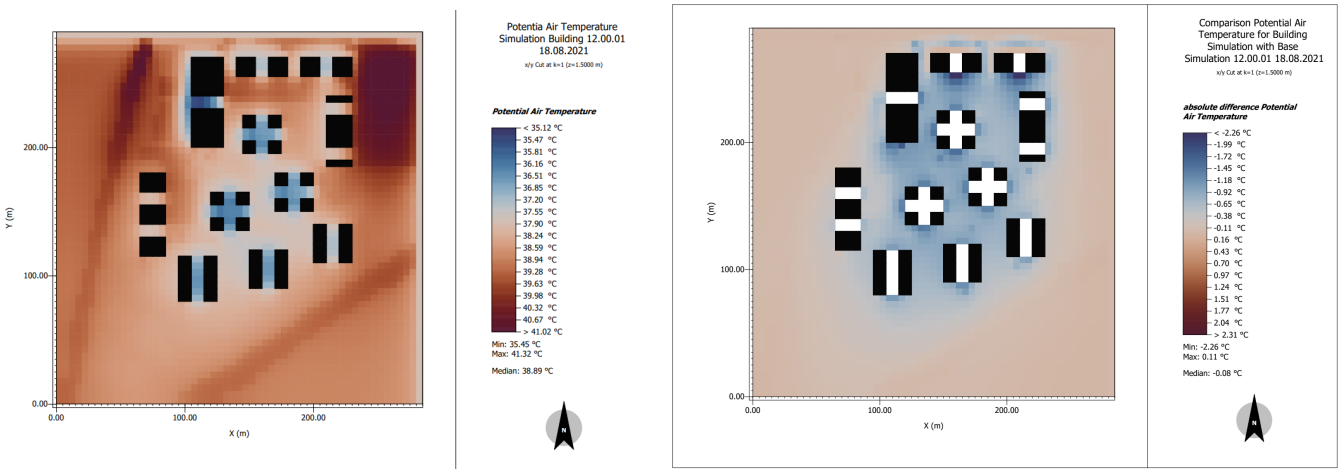

((a)) Simulation result ((b)) Comparison with base case

Figure 9: Potential air temperature diagram for the building modifications

A significant finding is the cooling observed in the urban canyon areas, which are predominantly shaded in blue. Temperature reductions in these zones reach up to 2.26^{o}C, a notable improvement that can substantially enhance the site's thermal comfort.

In contrast, the outer open areas show minimal or no change, with a maximum positive difference of 0.11°C. These small variations are likely within the margin of error of the simulation software and are expected since no modifications were implemented in these areas.

Anomalies were detected on the north facades of Buildings 2 and 3, where a thin strip fails to cool as much as the surrounding areas. This unexpected behavior merits further investigation to understand its underlying cause.

4.2 Surface temperature

In general, Figure 10 suggests minimal impact on surface temperatures, as most of the diagram displays values near zero (represented by a median shade light red).

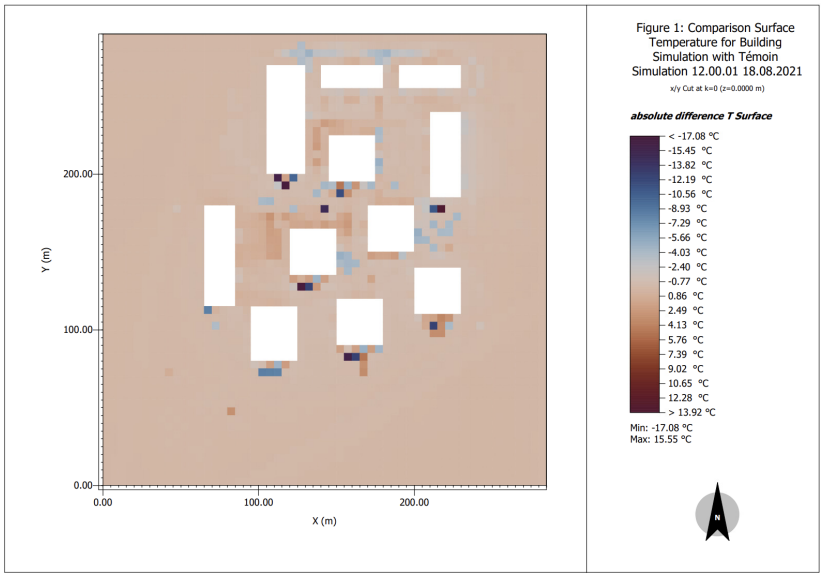

Figure 10: Surface temperature diagram for comparison of the building modifications with the base case

However, small variations are observed near the edges of the openings, likely due to localized airflow enhancements created by these design features. These openings are intended to improve ventilation, which may explain the slight surface temperature changes in their vicinity.

4.3 Wind

To start, a general positive impact is observed, with minimum and maximum wind speeds increasing by 0.01 m/s and 0.03 m/s, respectively.

The performance of the openings depends significantly on their orientation relative to the wind direction. When parallel to the wind, the openings create high-ventilation zones, particularly benefiting buildings near open areas such as Buildings 2, 3, 7, 10, and 11. In contrast, buildings located deeper within the urban cluster, like Buildings 5, 8, and 9, experience slower airflow through their openings due to wind encountering multiple obstacles before reaching them.

However, if the openings are perpendicular to the wind direction, as in Buildings 1, 4, and 6, they can become zones of low airflow. Depending on the surroundings, these areas may even develop into stagnation zones, potentially worsening thermal comfort locally.

As shown in Figure 11(b), the building modifications not only influence wind speed but also alter wind direction. This results in improved airflow in parts of the surrounding open areas, as indicated by the two shades of brown in the open zones on the diagram.

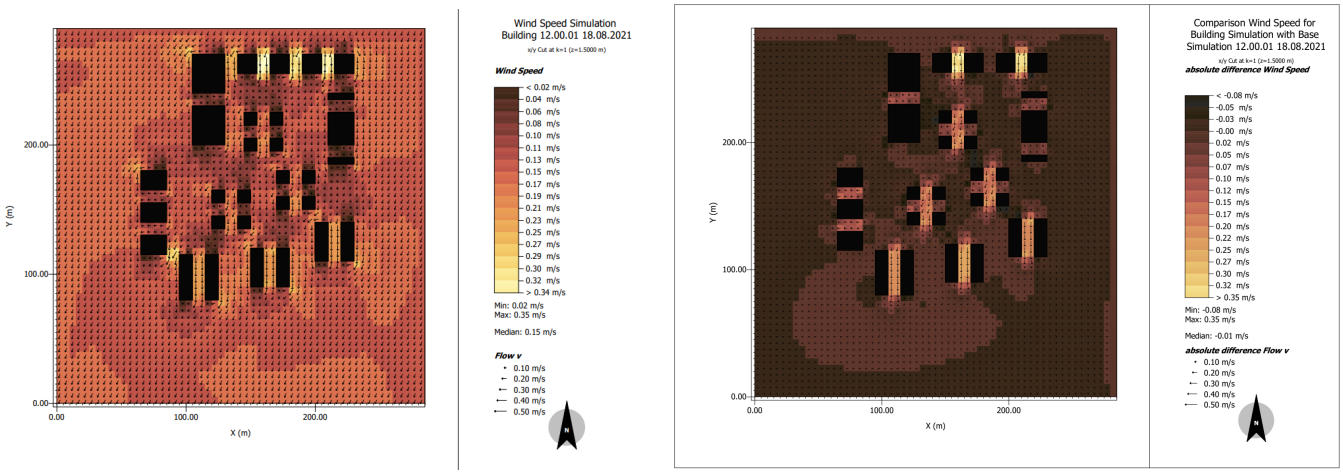

((a)) Simulation result ((b)) Comparison with base case

Figure 11: Wind diagram for the building modifications

4.4 Relative humidity

According to Figure 12(a), the openings are identified as humid zones, with Relative Humidity (RH) values reaching up to 63.83% (an increase of 3.51% compared with the base case). Variations in RH are observed both within individual openings and across different openings, likely due to the combined effects of wind patterns, solar radiation, and air temperature. It is important to note that while absolute humidity may remain constant, cooler temperatures result in higher RH levels.

Additionally, Figure 12(b) indicates a general increase in humidity across the urban cluster, with RH rising by up to 6.71%. This increase can be attributed to lower temperatures and the greening of facades and roofs introduced in the building modifications. Significant RH variations are particularly noticeable along the edges of the openings and on some building facades, reflecting localized impacts of shading, vegetation and temperature.

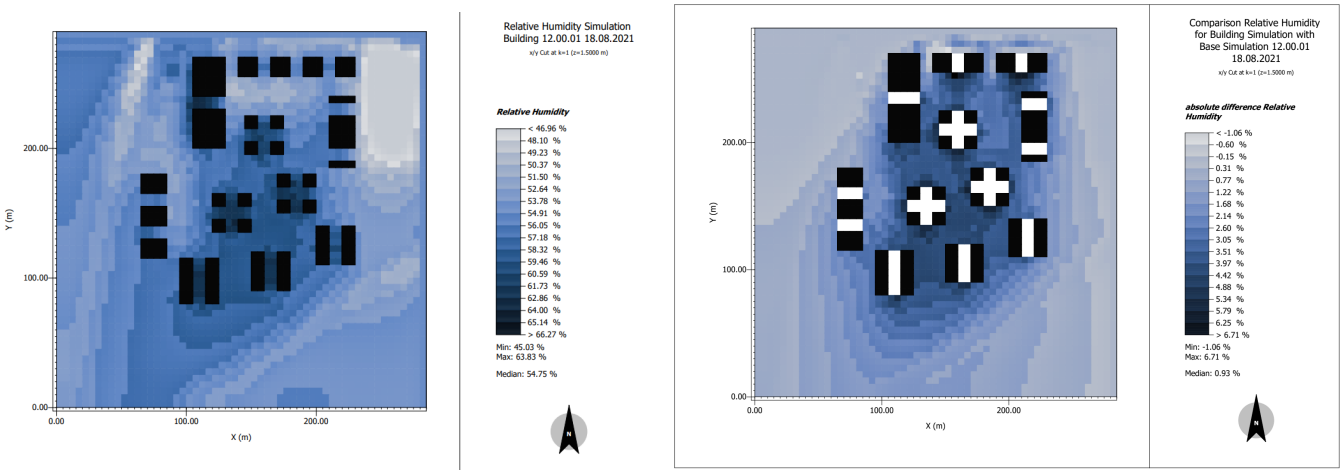

((a)) Simulation result ((b)) Comparison with base case

Figure 12: Relative humidity diagram for the building modifications

4.5 Radiation

As expected, the openings are zones with low reflected shortwave radiation levels due to the shading provided by the building tops, as the openings are only 4 or 5 m high, as seen in Figure 13(a). Within these zones, we observe a pixel of abnormality (a lighter shade of blue, indicating higher reflected radiation values) located in the northwest region of all three square buildings in the middle of the cluster. This could be caused by radiation entering through the openings.

In Figure 18(b) some changes are observed within the urban cluster. Notably, there is an increase in reflected radiation along the east facades of most buildings, with larger values observed for Buildings 2 and 3. Initially, we hypothesized that this effect might be related to the ivy or fumbia covered east walls. However, this increase is also present in buildings without an east green facades, suggesting a different cause. Additionally, some apparently random hotspots appear in orange/red on the diagram.

On the other hand, the edges of the north-south openings show a systematic decrease in reflected radiation, especially at the southern ends. This might be caused by increased airflow through the openings. Interestingly, the same effect is observed in openings oriented east-west, even though they have lower wind speeds. This suggests that the decrease in reflected radiation may instead be due to the absence of building material in these areas.

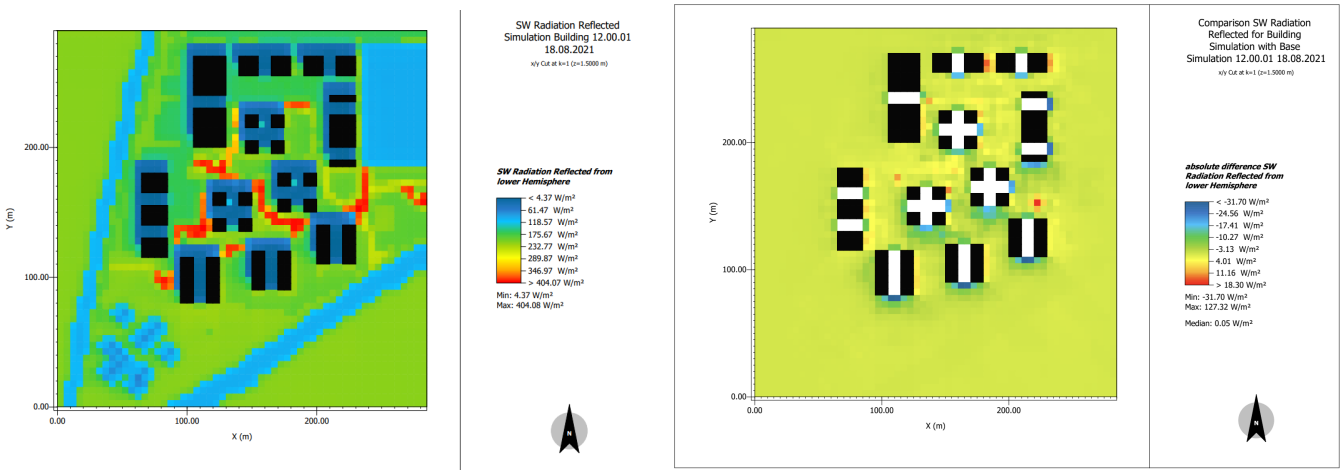

((a)) Simulation result ((b)) Comparison with base case

Figure 13: Wind diagram for the building modifications

4.6 Overall evaluation

Overall, the combination of greenery and building porosity appears to be an effective mitigation solution, as it successfully increases airflow and reduces air temperature. However, certain aspects, such as increased radiation in specific locations and wind speeds that remain relatively low, indicate that further refinements are needed to optimize the design.

5 Ground - Environment Interactions

The mitigation strategy consists in substituting the concrete paths connecting the buildings into gravel paths. Additionally, the parking lot, which was previously made of asphalt is turned into loamy soil. These modifications are expected to reduce the air and surface temperatures due to the following aspects:

- **Thermal properties**: The lower thermal diffusivity and conductivity of gravel and loamy soil compared to both concrete and asphalt means that the ground will store and release less heat. This results in an increase of the stability for surfaces temperatures and a decrease of the urban heat island magnitude.

- **Hydrological benefits**: Gravel and loamy soil allow water infiltration, reducing runoff and promoting groundwater recharge. This helps maintain the hydrological balance, whereas concrete and asphalt surfaces are largely impermeable and contribute to increased runoff. Additionally, water retained in pores of gravel or soil can evaporate, providing a cooling effect through latent heat transfer, unlike concrete, which lacks such moisture-retention capabilities.
- **Environmental interaction**: Gravel and loamy soil surfaces can better support vegetation growth due to water infiltration and the lower thermal interference, enhancing urban greening opportunities.

Following the completion of the simulations, the following comparison has been established with the base case.

5.1 Radiation

In the base case scenario, higher levels of reflected shortwave radiation were observed, particularly over asphalt and concrete areas. These surfaces, due to their lower albedo and higher absorption properties, concentrated peak values of radiation, leading to elevated heat retention. After modifications, there was a significant reduction in reflected shortwave radiation in areas converted to loamy soil and gravel. These new surfaces, with their higher albedo compared to asphalt and concrete, reflected more solar energy. This change reduced overall heat absorption in the area, which, in turn, lowered surface temperatures and mitigated urban heat island (UHI) effects. This improvement contributed to enhanced thermal comfort in the modified areas. For instance, in the base case scenario, peak reflected radiation reached 407.21 W/m^2, primarily over asphalt and concrete surfaces. After modifications, the peak reflected radiation decreased to 253.74 W/m^2 in areas where these surfaces were replaced with loamy soil and gravel.

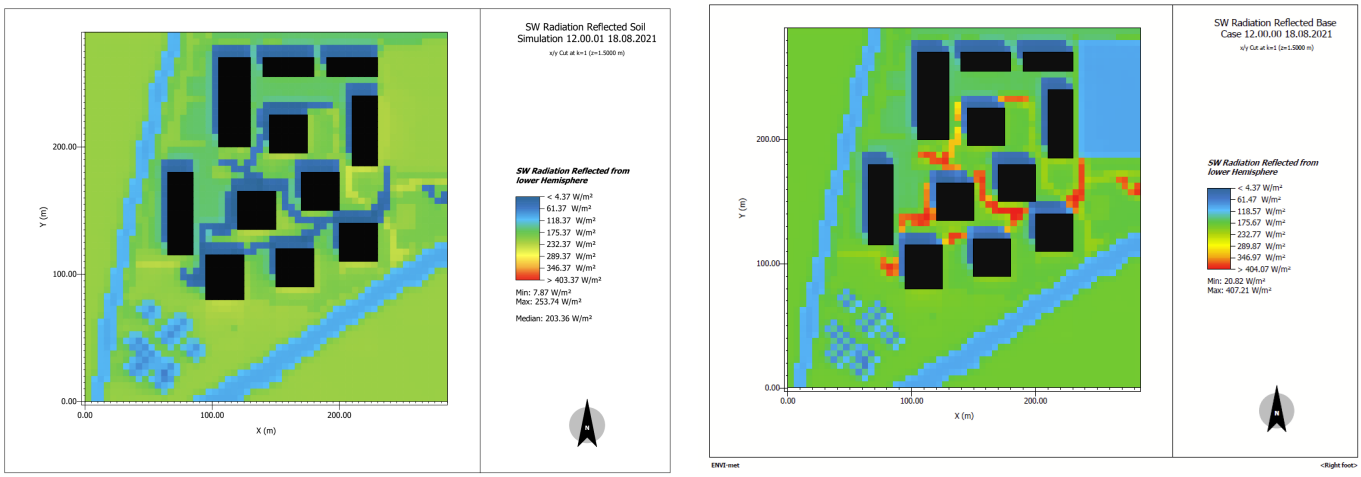

((a)) Simulation result

((b)) Comparison with base case

Figure 14: Radiation diagram for the ground modifications

5.2 Humidity

In the base case, relative humidity levels were notably lower, particularly in areas dominated by impermeable surfaces such as asphalt and concrete. These surfaces are less effective at retaining moisture, which contributes to drier microclimates and reduced atmospheric humidity. After the modifications, relative humidity levels increased in the areas where asphalt and concrete were replaced by loamy soil and gravel. These natural surfaces are better at retaining moisture, which enhances evapotranspiration processes. As a result, this change not only improved the localized microclimate by increasing atmospheric moisture but also led to cooling effects in the surrounding areas. The modifications to the soil produced a significant improvement in relative humidity levels, contributing to better thermal comfort and more effective regulation of the microclimate in the area. As an example, the relative humidity's values in the base case were as low as 46.96% in areas dominated by impermeable surfaces. After the modifications, relative humidity increased

significantly, with minimum values rising to 51.50% in areas where loamy soil and gravel replaced the previous surfaces. This change reflects an increase of 4.54% in minimum relative humidity, demonstrating the improved moisture retention and evapotranspiration capabilities of the modified soils.

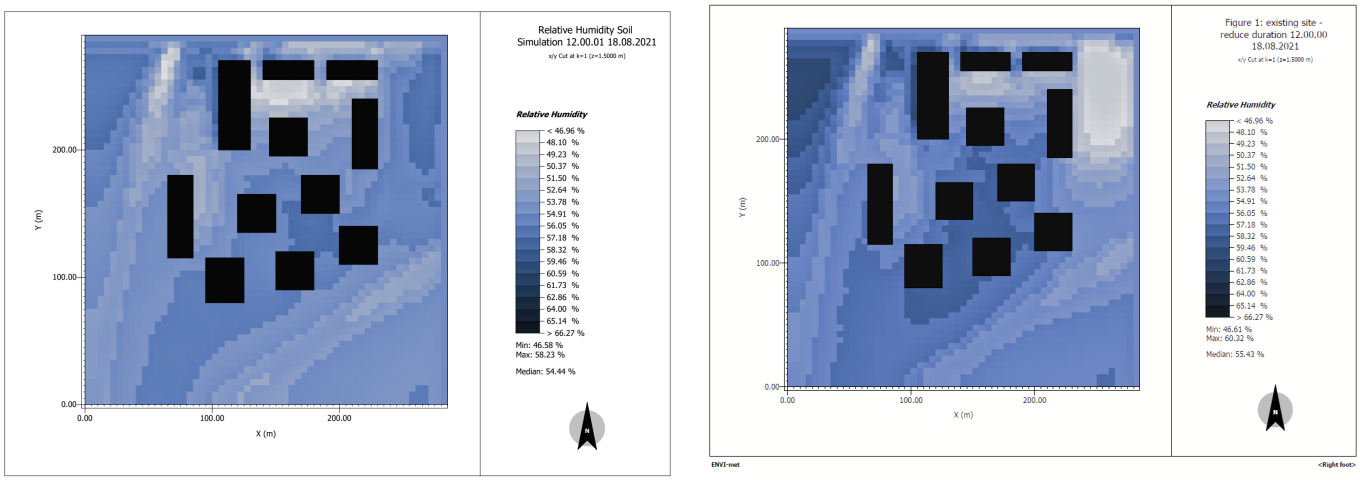

((a)) Simulation result ((b)) Comparison with base case

Figure 15: Relative humidity diagram for the ground modifications

5.3 Wind speed

In the base case, wind speeds were generally lower near buildings and in areas dominated by impermeable surfaces. High temperatures generated by asphalt and concrete surfaces caused convective currents, which potentially disrupted localized wind flow and reduced wind movement in these zones. After the modification, wind flow patterns exhibited marginal improvement, particularly in areas where the soil had been altered. The reduced heat emission from the loamy soil and gravel contributed to air stabilization, allowing for more uniform wind flow. However, the changes in wind speed were less significant when compared to other parameters affected by the modifications. This adjustment thus provided a minor but noticeable improvement in the uniformity of wind distribution across the area. Indeed, wind speeds in the base case reached minimal values of 0.01 m/s near buildings and asphalt surfaces. After modifications, wind speeds improved slightly, with minimum values increasing to 0.02 m/s in the modified zones. Although the change represents only a marginal increase of 0.01 m/s, it indicates a stabilization of airflow patterns, likely resulting from reduced thermal convection in these areas.

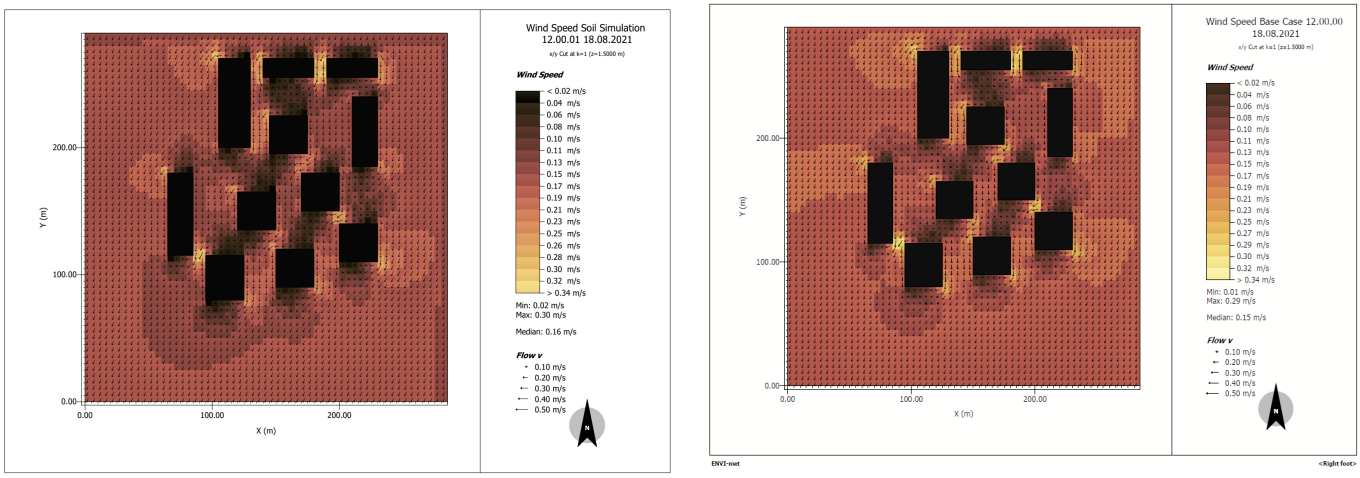

((a)) Simulation result ((b)) Comparison with base case

Figure 16: Wind speed diagram for the ground modifications

5.4 Surface temperature

In the base case, surface temperatures were significantly higher in areas covered by asphalt and concrete. This was due to the low albedo and high thermal mass of these materials, which absorbed and retained heat, thereby contributing to the formation of pronounced heat islands. After the modifications, surface temperatures decreased considerably in the areas where soil was changed. The introduction of loamy soil and gravel, which possess lower thermal mass and higher moisture retention, reduced heat absorption. This change promoted cooling through increased evapotranspiration. For instance, surface temperatures reached a maximum of 49.15°C in the base case. Following the modifications, these temperatures decreased to a maximum of 41.38°C in areas where loamy soil and gravel replaced the original surfaces. This reflects a reduction of 7.77°C in maximum surface temperature, highlighting the cooling effect of these permeable and thermally efficient materials.

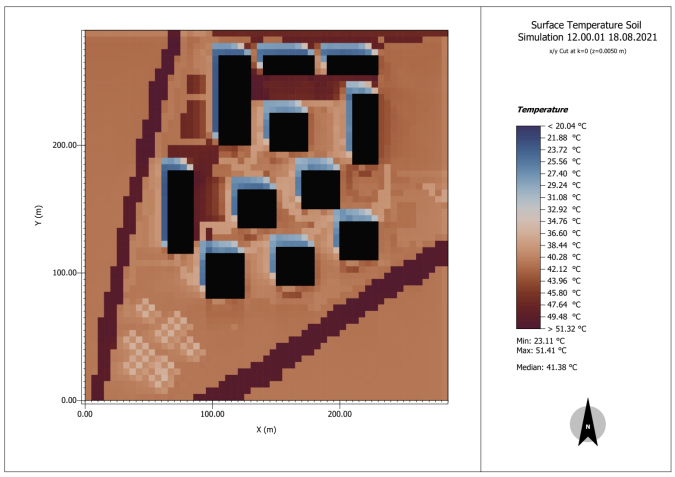

((a)) Simulation result

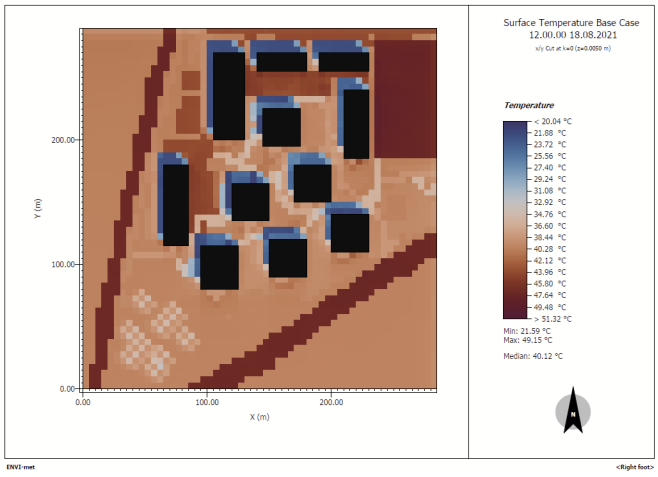

((b)) Comparison with base case

Figure 17: Surface temperature diagram for the ground modifications

5.5 Air temperature

In the base case, elevated air temperatures were recorded above asphalt and concrete surfaces. These materials contributed to localized heat islands due to their high heat capacity, which intensified the surrounding air temperature. After the modifications, air temperatures significantly decreased in areas where the soil was altered. The cooling effect of loamy soil and gravel, facilitated by their higher albedo and the process of evapotranspiration, played a crucial role in reducing air temperatures. This notable improvement in air temperature is critical for enhancing urban thermal comfort and mitigating the effects of urban heat islands. Air temperatures were also elevated in the base case, with a maximum of 40.65°C recorded above asphalt and concrete surfaces. After the implementation of soil modifications, it got reduced to a maximum of 38.75°C over the altered areas. This corresponds to a decrease of 1.90°C.

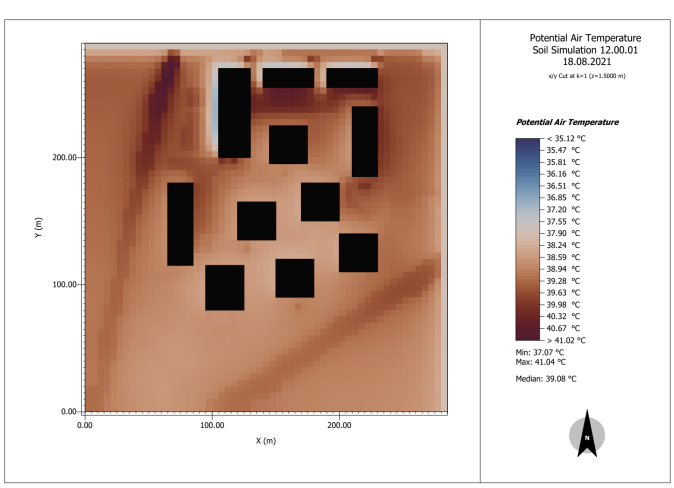

((a)) Simulation result

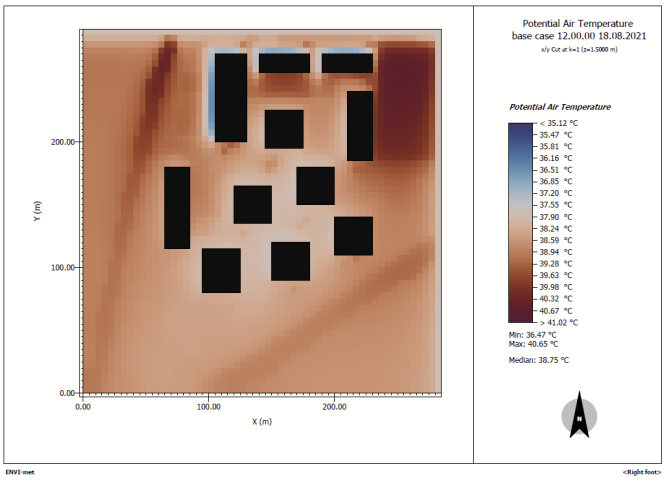

((b)) Comparison with base case

Figure 18: Air temperature diagram for the ground modifications

6 Water body - Environment Interaction

To investigate the effect of two water bodies in relation to the buildings and the Urban Heat Island (UHI) effect, one pond was placed between the buildings and another west of the buildings. Both ponds have a surface area of 450m^2 and a depth of 2m. This setup was designed to analyze the difference in cooling effects resulting from the placement of the water bodies. In order to model the water bodies, "deep water" was chosen with an albedo value of 0 and an emissivity of 0.9 W/m^2. The layout is visible in figure 19.

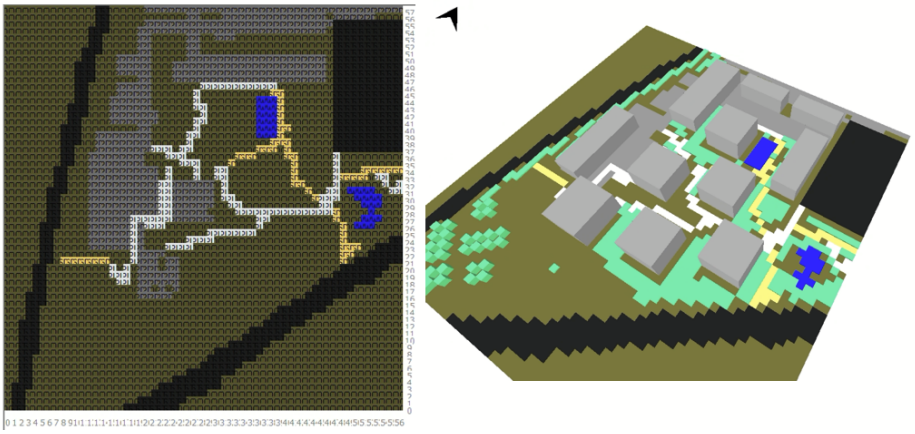

Figure 19: Model for the water body modification.

Water bodies (blue areas) can contribute to the mitigation of Urban Heat Islands (UHI) through the physical process of water evaporation (9). They exhibit thermal inertia, where the peak temperature is reached with a delay relative to the peak air temperature, and the atmosphere above blue bodies is generally temperate due to the high heat capacity of water (MJ m^{-3} K^{-1}). Furthermore, relatively large water bodies have higher cooling effects than equally distributed water bodies due to their greater thermal inertia and lower surface-area-to-volume ratio.

Water has a high heat capacity, meaning it can absorb and retain heat efficiently. Additionally, a smaller surface-area-to-volume ratio minimizes heat loss through evaporation or radiation compared to multiple smaller bodies, which have relatively more surface area exposed to the environment. This allows the large water body to maintain and dissipate heat more effectively over time.

Water bodies can be characterized by a shape factor called landscape shape index (LSI, 2). In the modified version, the rectangular water body located between the buildings has a LSI of 1.2 and the second water body located to the west of the buildings has a LSI of 1.9. A higher Landscape Shape Index (LSI) value means that the water body has a more complex, irregular shape, while a lower LSI value indicates a simpler, rounder, or more regular shape. Studies have shown that lower LSI values indicating regular shaped water bodies tend to have a more efficient cool air dispersion which leads to higher cooling effects and more even water temperature distributions (8). Therefore regular shapes were used in the model on ENVIMET.

$$LSI = \frac{P}{2\sqrt{\pi * A}} \tag{2}$$

Where P is the perimeter and A is the area of the water body.

6.1 Potential air temperature

A cooling effect due to evaporative cooling is to be expected thanks to the added water bodies (10). As it is observed in 20 no significant change can be observed by singly comparing the two graphs. But figure 21 shows that the two water bodies have an impact on the surrounding air temperature. It can be observed that the water bodies between the buildings contribute more to cooling. This was expected, as the temperature in those areas was higher initially. The legend displays positive values because the difference from the base case to the water bodies is depicted, which means that the temperature difference for decreasing temperatures is shown as positive. Therefore, it can be concluded that it is more efficient to place the water bodies between the buildings rather than outside.

However, the cooling effect is not very significant. This could have various causes. It could be because the reference height is 1.5 m, where the effect is already smaller, or because the discretization of 5 m × 5 m is not fine enough. However, when the reference height is lowered to 0.5 m, the simulations show that the relevant areas are covered by vegetation. This might have a predominant influence on the potential air temperature. Another potential reason we don't see significant changes could be that the total added water bodies' surface is 900 m^2, while our total neighborhood has a surface area of 84100 m^2. The water bodies added in this model, therefore, represent only a tiny 1% of the entire surface. Adding a greater water surface might bring more noticeable changes in temperature. Hence, the extent of the changes, as well as their type, plays an important role!

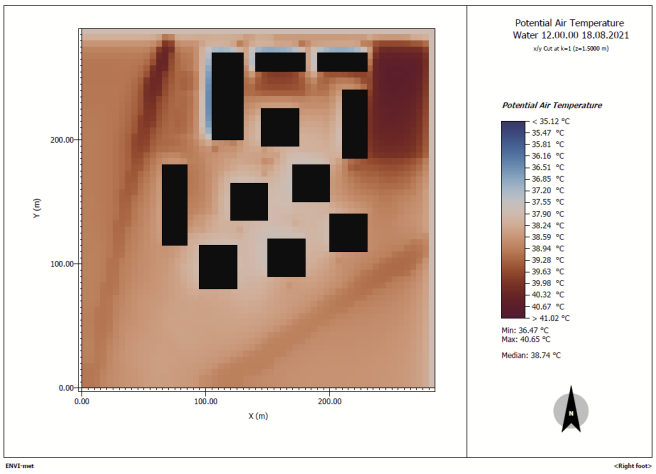

((a)) Simulation result

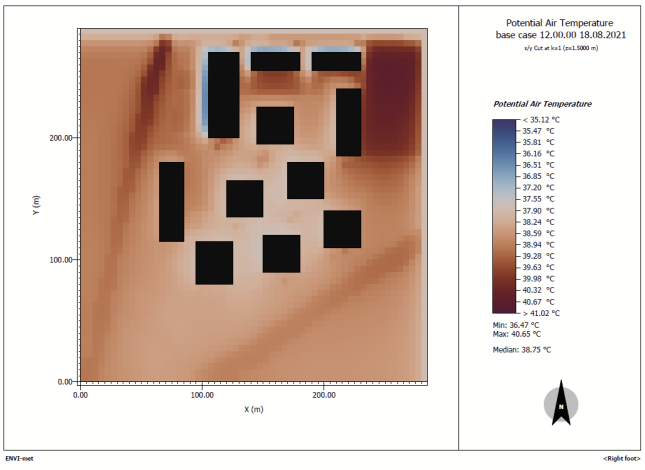

((b)) Comparison with base case

Figure 20: Potential air temperature diagram for the water body modification

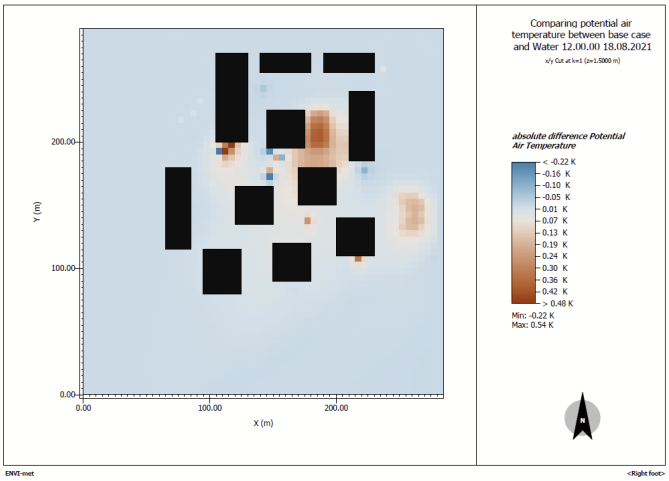

Figure 21: Comparison of potential air temperature for base case and water body modification

6.2 Relative humidity

Water bodies in urban regions are expected to increase relative humidity, especially downwind of the water bodies (11). However, similar to the potential air temperature, no significant change in relative humidity was observed in this case as seen in figure 22. Figure 23 shows a maximal increase in relative humidity at the location of the two water bodies. The maximal difference is equal to 0.86% and corresponds to the water body between the buildings. But as it is so small it is considered as insignificant. As the values are so small it is possible that the vegetation, which is displayed as being lower than 1.5 m in the simulation, distorts the results.

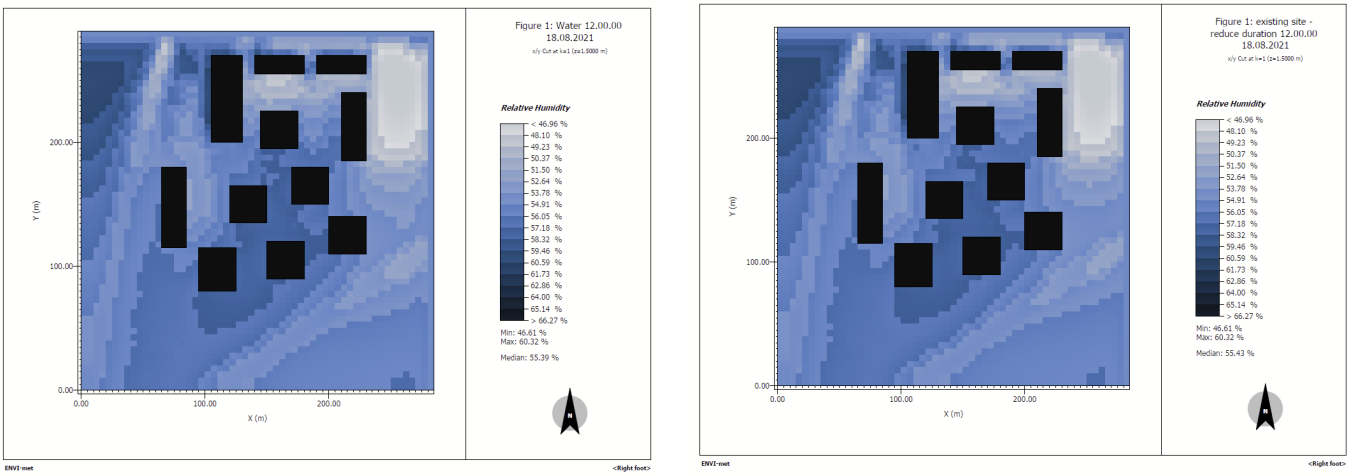

((a)) Simulation result

((b)) Comparison with base case

Figure 22: Relative humidity diagram for the water body modification

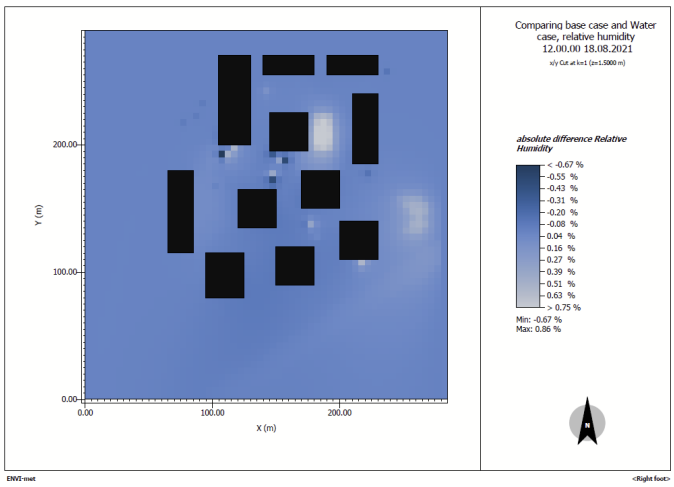

Figure 23: Comparison of relative humidity for base case and water body modification

6.3 Surface temperature

The surface temperature has changed in comparison to the base case only at locations where water bodies were placed, but at these locations, the change is significant. The new surface temperature represents the minimum temperature in the simulation, reaching 20.11°C, while the same location previously exhibited a surface temperature of 38.5°C. This indicates the importance of water bodies when aiming to reduce the UHI effects. In terms of surface temperature, no difference is observed between the water bodies. The difference is shown in figure 25. It can be observed that the maximal difference is equal to 22.12K for the two water bodies whereas the influence on the surrounding is minimal. Some small spots exhibit an increase whereas others show a decrease in surface temperature. This phenomenon is observed rather downwind of buildings. This phenomenon could be attributed to the cooling effect of water bodies combined with wind, which increases evaporation. However, since there is primarily one point that becomes noticeably warmer right next to another point that cools down, this could also be a result of the model's relatively coarse spatial discretization.

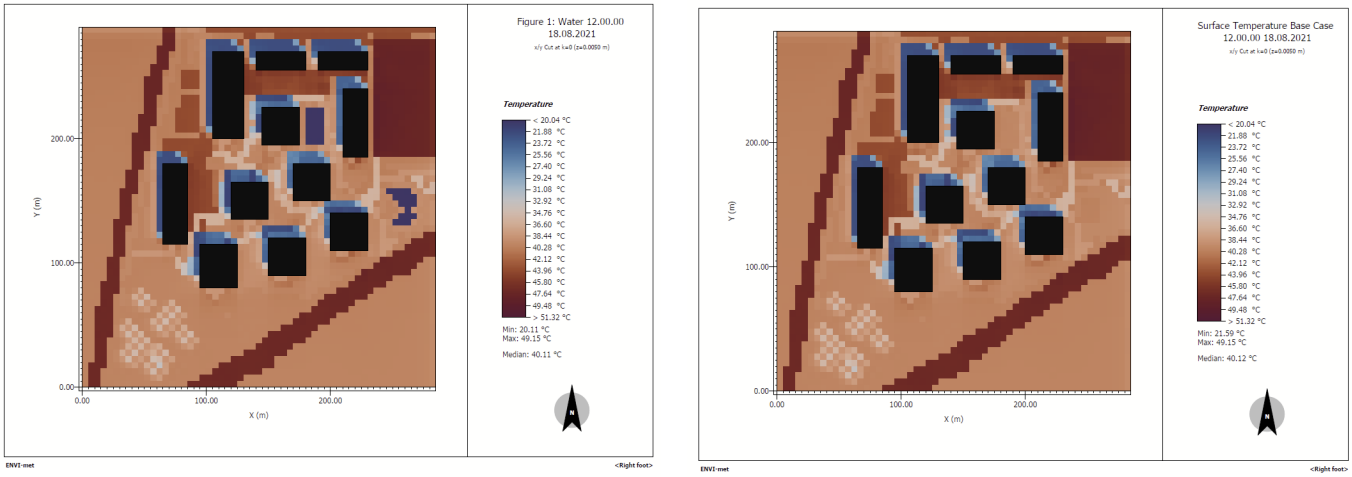

((a)) Simulation result

((b)) Comparison with base case

Figure 24: Surface temperature modification for the water body modification

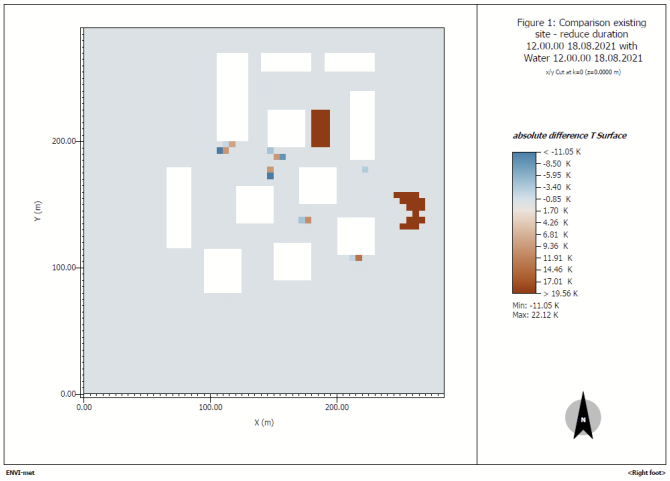

Figure 25: Comparison of surface temperature for base case and water body modification

6.4 Wind

The wind speed remains virtually unchanged compared to the base case, as expected, given that water bodies do not function as obstacles to wind flow and has a negligible roughness.

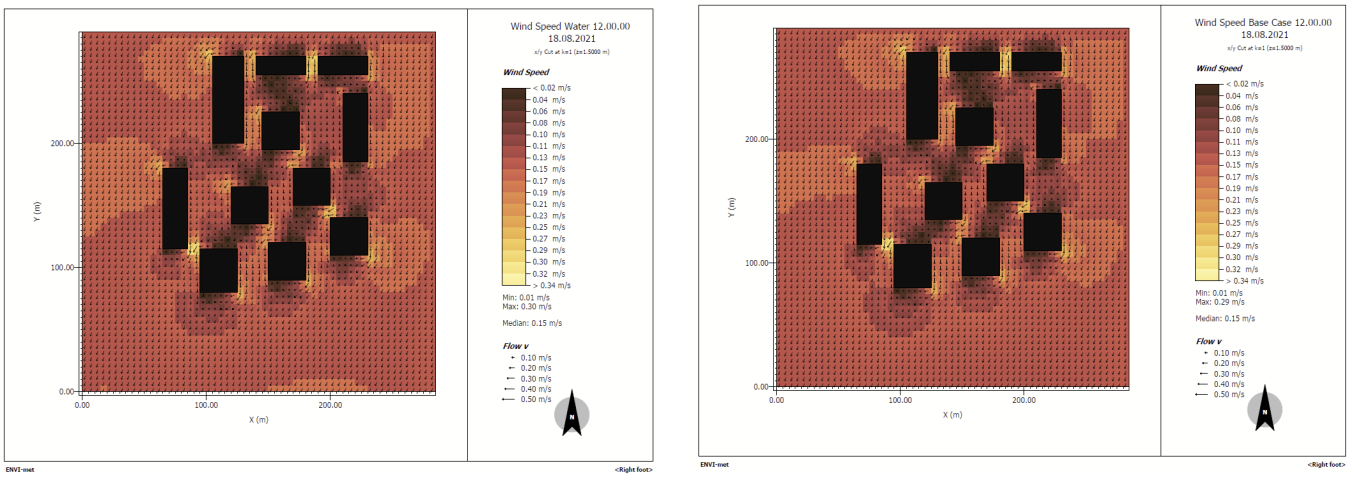

((a)) Simulation result

((b)) Comparison with base case

Figure 26: Wind diagram for the water body modification

6.5 Radiation

Studies have shown that water bodies are very efficient in absorbing radiation. Due to the high thermal capacity, much heat can be absorbed with little increase in the water temperature (9). The radiative properties of water depend on the angle of incidence of the light and the water depth. The percentage of radiation absorbed increases with water depth, and water is generally transparent to shortwave radiation. The reflectivity depends solely on the solar incident angle, which in the simulation is at zenith. Therefore, the simulation shows the water bodies at their minimum reflectivity, and maximal absorption is expected. As the water bodies consist of ponds, the turbidity is expected to be low (modeled as 2.1 NTU), and therefore less radiation is scattered. The obtained results are shown in figure 27.

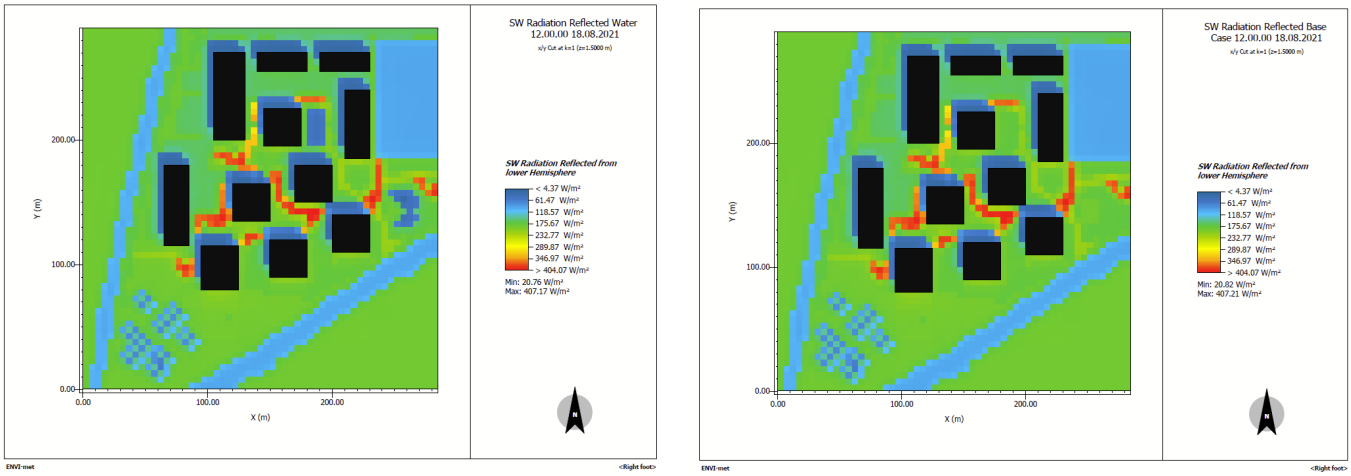

((a)) Simulation result

((b)) Comparison with base case

Figure 27: Radiation diagram for the water body modification

In this case, ponds with a water depth of 2m were simulated in areas that previously had a surface material consisting of sandy loam with an albedo of 0.2. As a result, less shortwave radiation is reflected in the modified scenario at the locations of the two water bodies. In average, both ponds show a shortwave reflection of around 20 W/m^2 but the less uniformly shaped pond shows a less uniformly distribution of reflected shortwave radiation.

7 Vegetation - Environment Interaction

Vegetation is an essential component of urban environments, playing an important role in regulating micro climates, improving air quality, and mitigating the Urban Heat Island (UHI) effect. Studies have shown that trees are more effective than grass in terms of urban cooling (12). Therefore, a model layout was chosen that features many trees in order to maximize the cooling effects as can be seen in figure 28.

In order to investigate the influence of different configurations of urban greenery, the current situation (base case) is compared with a modified version. The current situation shows small lanes of vegetation between the buildings and a small urban woodland close to the roads. Additionally there are some trees close to the parking lot. The modified version includes significantly more vegetation, the biggest change is underground parking, the current parking lot has been replaced by a grassy area with several trees. In the western part between the buildings of group A and B, bushes were added and some were also added to the south of the former parking lot.

Grass on asphalt would not be practically possible.

However, it must be noted that the floor has not been changed in this modification. This means that the grass on the parking lot in the simulation is still planted on asphalt. The actual effect is therefore only visible in the combined modification when the ground modification is combined with the vegetation modification. The layout of the vegetation modification is visible in figure 28.

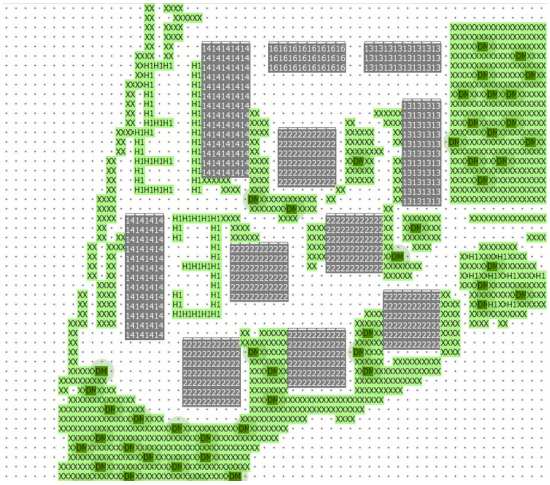

Figure 28: Vegetation modification model

Trees ("DM") are the most effective in reducing urban temperatures due to their extensive canopy coverage, high leaf area index (LAI), and ability to block solar radiation, lowering surface and air temperatures. Their high rates of evapotranspiration release latent heat, further cooling the surroundings. Additionally, the height and density of their canopies reduce wind speeds and create stable micro climates. However, it is important to note that these positive effects only occur when the vegetation is not under water stress.

Bushes ("H") offer intermediate shading and cooling, making them ideal for compact spaces such as near facades or in narrow streets. While less effective than trees, bushes still reduce wind speeds and enhance local thermal comfort. They also provide shading and contribute to evapotranspiration, helping to cool their immediate surroundings. In the simulation, Hedges with a height of 1m and an albedo value of 0.2 were chosen.

Grass ("X") primarily contributes to cooling through evapotranspiration, efficiently reducing ground-level surface temperatures. While it lacks the shading capabilities of trees and bushes, grass is highly effective in covering large areas. It is much better in water absorption and retention than asphalt. In the simulation, grass with a height of 25cm was chosen.

7.1 Potential air temperature

It is clearly visible in figure 29 that the potential air temperature decreased over the area of the former parking lot. In the base case, temperatures exceeding 40.0°C were simulated at the former parking lot (reference: 1.5 m above ground), whereas in the modified version, the average temperature is approximately 39.5°C. However, since the ground in the simulation remains asphalt, the cooling effects are underestimated. The potential air temperature between the buildings has increased by an average of 1°C, which can be attributed to the reduced wind speeds. Furthermore, the modified vegetation simulation does not yet reflect the full effect of vegetation, as the ground surface has not been altered (this is addressed in the ground modification simulation). Therefore, the true impacts can only be observed in the combined simulation.

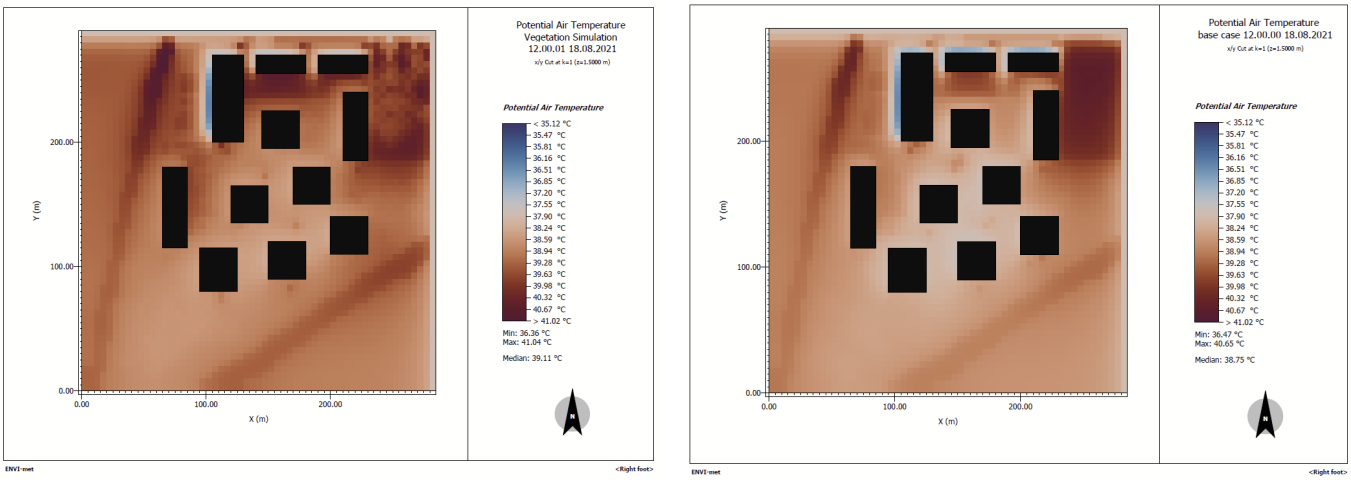

((a)) Simulation result ((b)) Comparison with base case

Figure 29: Potential air temperature diagram for the vegetation modification

7.2 Relative humidity

A general increase in relative humidity can be observed compared to the base case (figure 30). The biggest difference is visible on the parking spot where the relative humidity increased in average by 2-3%. As the floor has not yet been modified, the combined case is expected to increase the relative humidity even more as the soil can retain more water.

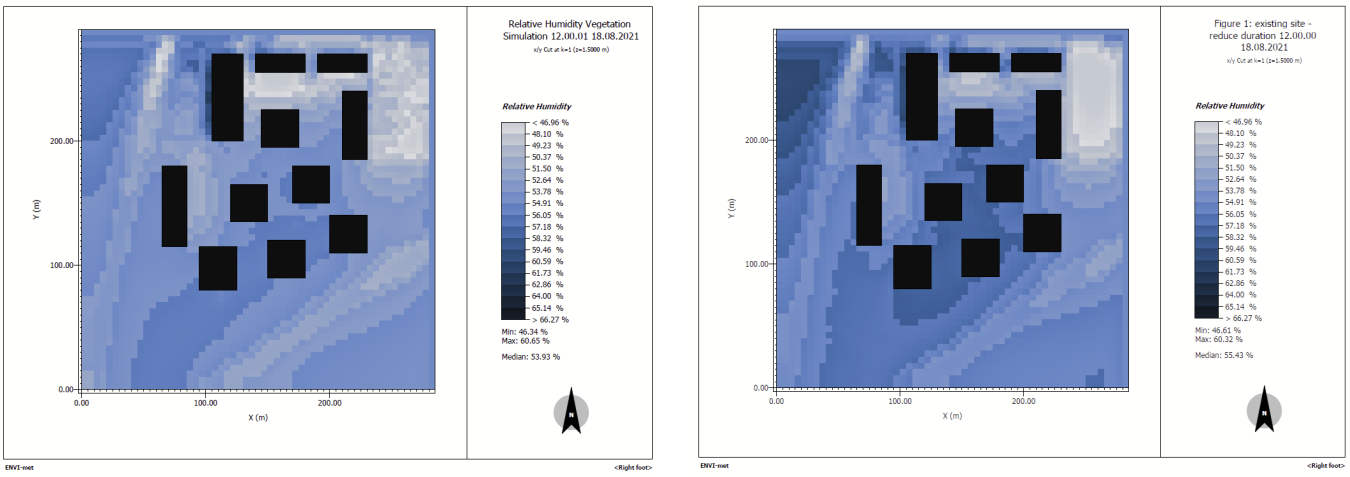

((a)) Simulation result ((b)) Comparison with base case

Figure 30: Relative humidity diagram for the vegetation modification

7.3 Surface temperature

The difference is most significant for surface temperatures. As can be observed in figure 31 and 32 the temperature decreased due to the vegetation modification especially where trees were added but also the hedges contributed to the cooling effect. Here it is important to note that on figure 32 the decrease in temperature has a negative sign. While the base case shows uniform temperatures of over 49°C in the parking lot, the surface temperature in the modified version varies between 33°C and 45°C thanks to the added trees. The surface temperature has also decreased in the west between the buildings where bushes have been added. However, the difference is smaller than in the parking lot, averaging about 3°C less. In the southwest, the lawn and the additional trees reduce the surface temperature. Although the temperature difference is only around 2°C, the affected area is significantly large and it is an improvement in terms of cooling compared to the base case, where the urban forest was simulated with only 9 trees.

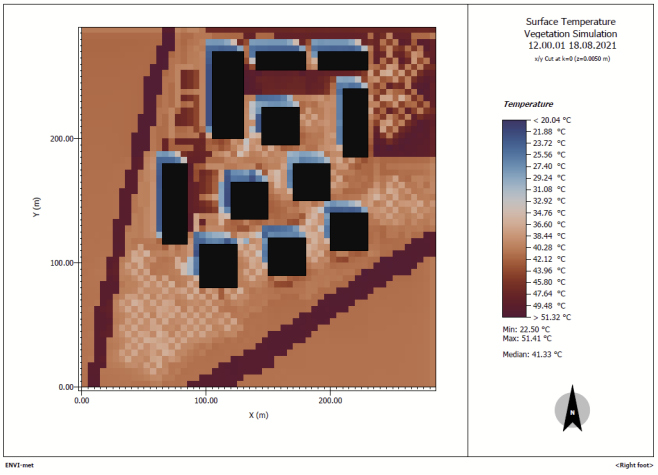

((a)) Simulation result

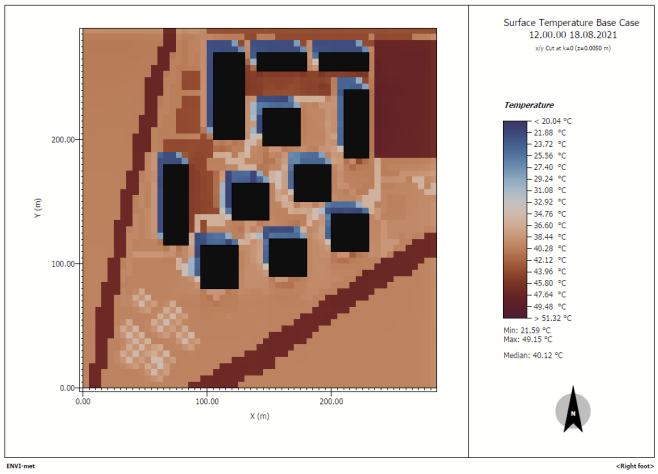

((b)) Comparison with base case

Figure 31: Relative humidity diagram for the building modifications

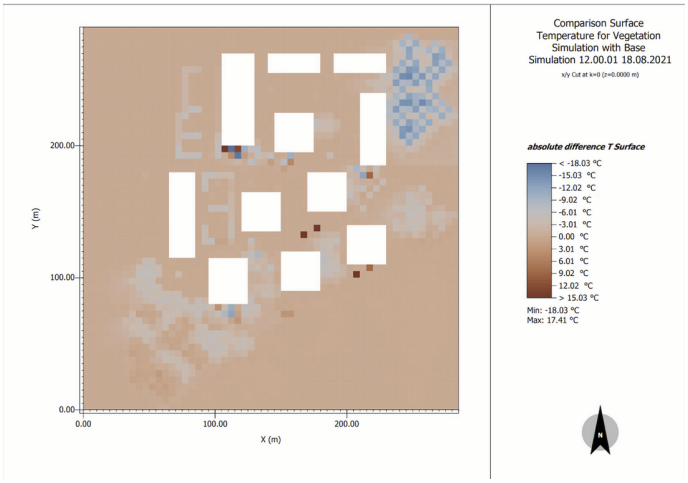

Figure 32: Comparison of surface temperature for base case and vegetation modification

7.4 Wind

Both simulations (figure 33) display low flow velocities (< 0.20 m/s) dominating most of the domain, but the modified case shows slightly decreased flow vectors in regions of vegetation, such as on the parking lot and in the southwest of the buildings where trees and grass were added. The vegetation acts as a wind barrier to the wind coming mostly from the north of the buildings. This vegetation shield forces the wind to pass by the sides or higher up than the reference height of 1.5 m above the ground. Even though wind speeds between the buildings have decreased, some building corners exhibit elevated wind speeds ($>$0.34 m/s). Even though the vegetation acts as a barrier, the vegetation layout in the modified scenario includes gaps and lower-density areas, and wind can be funneled through these spaces. This channeling effect leads to localized increases in wind speed as wind can accelerate around the edges of vegetative obstacles or over the top where the vegetation is not continuous or tall enough.

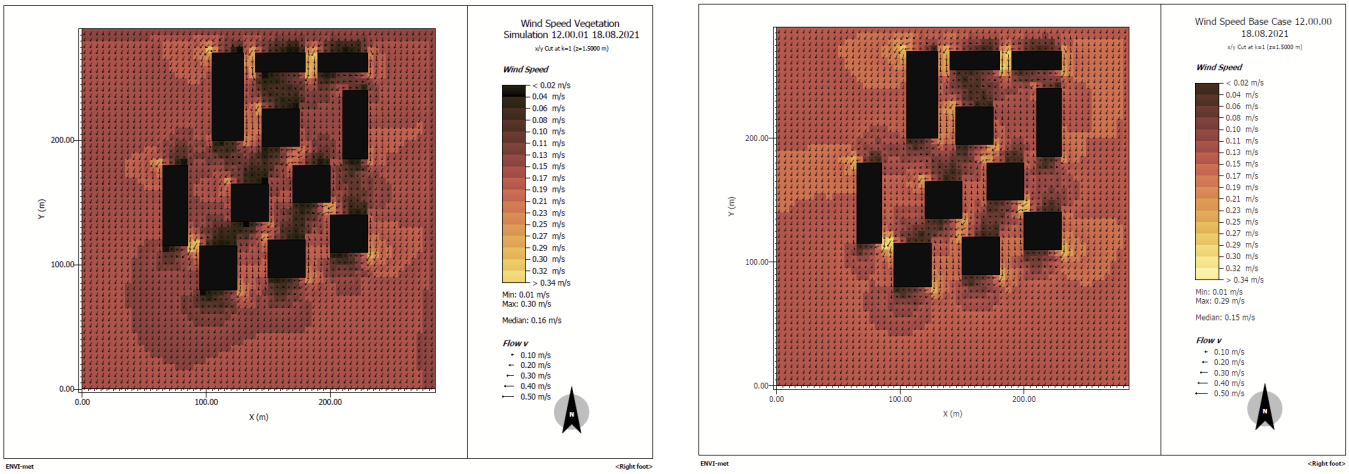

((a)) Simulation result ((b)) Comparison with base case

Figure 33: Wind diagram for the vegetation modification

7.5 Radiation

Based on the reflected shortwave radiation simulation (figure 34), it can be observed that the vegetation reflects significantly less radiation. Compared to the base case, the outlines of the vegetation are clearly visible on the former parking lot and in the southwest of the buildings. While the average reflected radiation was previously 118 W/m^2 and 175 W/m^2, in the modified scenario, areas where trees were planted reflect less than 60 W/m^2.

This may be due to the shading effect (less SW radiation reaching ground) of trees rather than surface smoothness.

Although asphalt has a low albedo, ranging between 0.05 and 0.27 (in the simulation 0.12), it appears more reflective than trees (albedo of 0.2) and grass (albedo of 0.2) in this simulation. This could be due to the fact that asphalt surfaces are much smoother and more uniform, and are modeled in an idealized manner in the simulation. Additionally, the specific type of vegetation is not precisely defined in the simulation. This shows that vegetation contributes to thermal comfort not only by providing shade but also by reducing the amount of reflected solar radiation. This effect is also supported by literature (13).

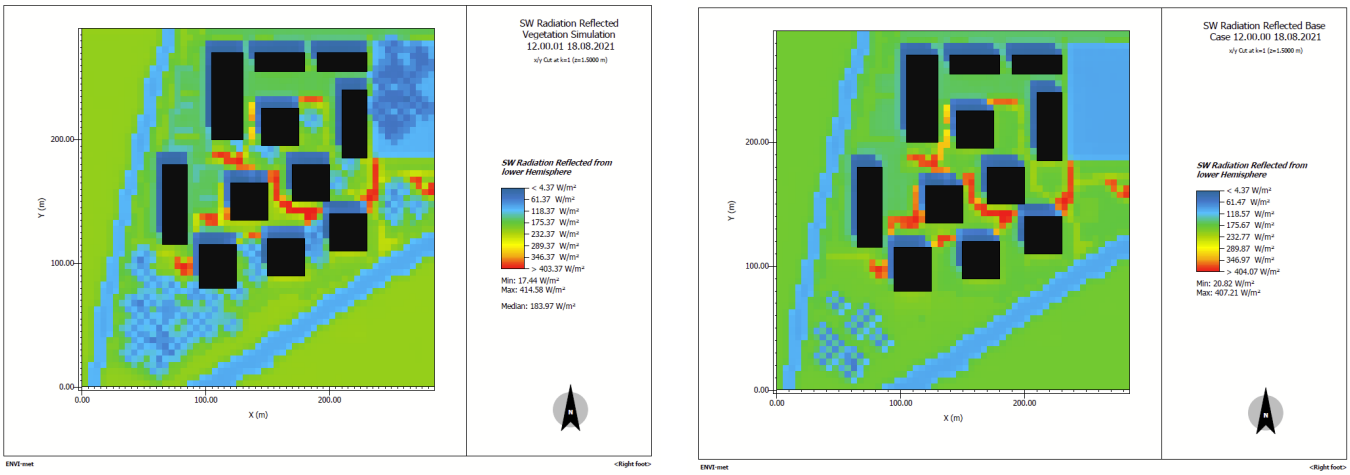

((a)) Simulation result ((b)) Comparison with base case

Figure 34: Radiation diagram for the vegetation modification

8 Energy Balance

For each simulation, two graphs were plotted to study the influence on the energy balance, each showing the energy variation throughout the day. In order to get an idea of the energy balance, the two points showing

maximal respectively minimal latent heat flux were chosen for each modification and further analyzed.

For urban regions, the energy balance also includes the anthropogenic heat, but as the model does not take into account cars and humans, the anthropogenic heat cannot be extracted from the simulation. The energy balance is therefore simplified to the rural surface energy balance:

$$Q^* = Q_H + Q_{LE} + Q_G \quad (\mathrm{W/m^2})$$

where

Q^* : Net allwave radiation heat flux

Q_H : Sensible heat flux

Q_{LE} : Latent heat flux

Q_G : Ground heat flux (conduction to the soil)

The region of Ecublens is not considered a rural area; however, it is also not located in a highly urbanized region. Compared to major cities such as Zurich or even New York, the EPFL campus resembles a rural area more than an urban one. Therefore, this simplification is considered as acceptable.

8.1 Energy balance for the Base Case

At noon, the latent heat flux (Q_{LE}) varies between 0 and 365 W/m^2. It is observed that, for the point taken as maximum energy, the peak of LE is at noon, while for the point of minimum energy, the noon value is zero, but it varies throughout the day, reaching the peak at 4:00 pm with 200 W/m^2. This quantity is associated with water vapor transport; a negative value is expected only in the case of dewfall, which does not happen in this scenario.

On the other hand, the sensible heat flux (Q_H) is associated with the difference in temperature between the surface and the atmosphere. At noon, the values range between 0 W/m^2 and 90 W/m^2. Therefore, at noon, the Bowen ratio (β) < 1, and thus the latent heat dominates, keeping the surface and the lower atmosphere cooler while adding humidity to the environment. This can be observed by comparing the maximum values in the surface temperature diagram (Figure 4) and the air temperature diagram (Figure 3), as well as the good humidity values on average across the site. It is important to observe that the Bowen value does change throughout the day, as it reaches a value > 1 at 4:00 PM at the maximum energy point, for example, when Q_H reaches its maximum value of 275 W/m^2.

Finally, it is observed that the soil heat flux alternates between positive values at the start of the day and negative values at the end of the day, implying that heat is released from the surface at night. This effect can be observed through the lower surface temperatures in the midnight analysis (in Annex A.1.1).

It can also be observed that the net radiation is positive (reaching approximately 530 W/m^2) until approximately 6:00 PM and becomes slightly negative (reaching approximately -70 W/m^2 at 8:00 PM at the minimum energy point) afterward. As expected, heat is absorbed during the daytime and released during the night.

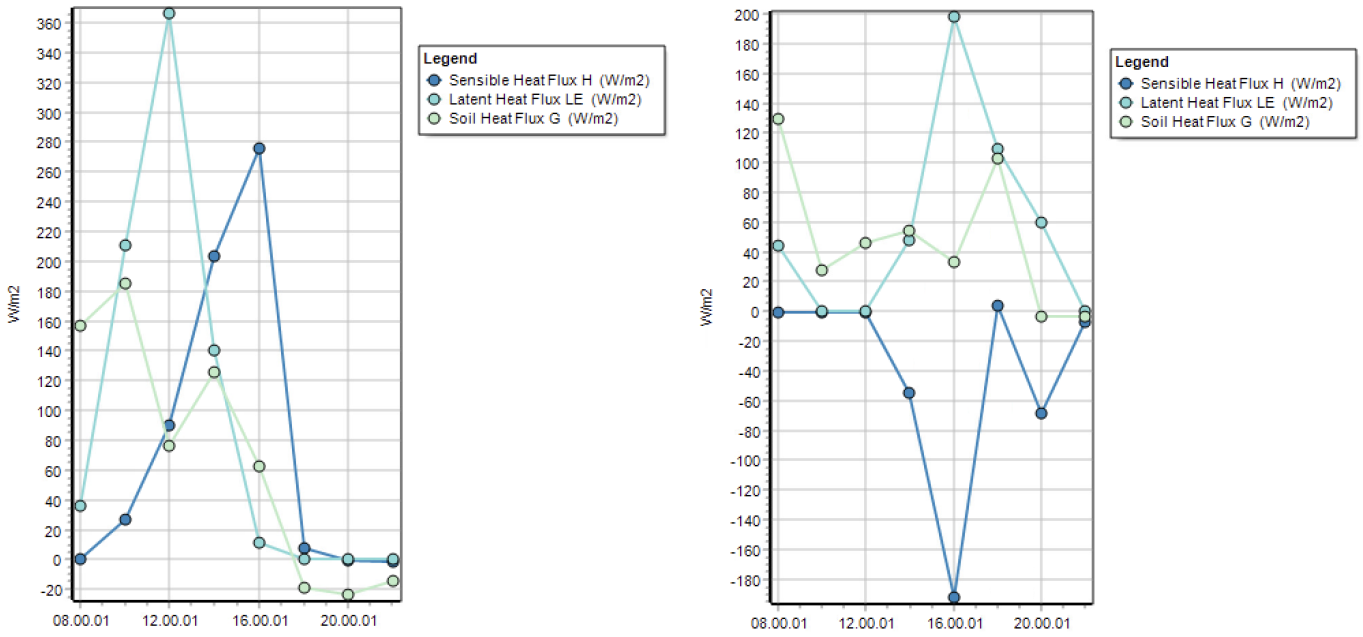

((a)) Maximal latent heat

((b)) Minimal latent heat

Figure 35: Energy balance for the base case

8.2 Energy balance for the Building modification

We start by analyzing the minimum energy point, and we observe an increase in values, which implies that more energy is being released from the surface to the atmosphere and into the ground. For example, the leak of the soil heat flux increases from 130 W/m^2 to 440 W/m^2 and is shifted from 8:00 AM to 10:00 AM. In addition, the peak of latent energy increases to 385 W/m^2 and is shifted to 12:00 PM (instead of 200 W/m^2 at 4:00 PM), implying that more water vapor is released into the atmosphere, leading to an increase in humidity (as corroborated by the earlier discussion). Although the increase in humidity is beneficial, analyzing the values at noon shows that the net radiation absorbed increases from 45 W/m^2 to 550 W/m^2. While this might seem negative initially, only 50 W/m^2 contributes to an increase in temperature (sensible heat), with the vast majority directed toward latent heat flux, which mitigates overheating by promoting evaporation and increasing humidity.

For the maximum energy point, we observe no shift in the latent peak, although there is an increase in the value from 365 W/m^2 to 540 W/m^2 (at noon). Nevertheless, the net radiation remains the same (530 W/m^2), meaning the energy absorbed by the surface is unchanged but is distributed differently. For instance, the soil heat flux (Q_G) becomes negative (-55 W/m^2), indicating that heat is absorbed by the surface from the substrate. The maximum sensible heat flux (Q_H) remains at 4:00 PM; however, we observe lower values.

Higher values of latent heat flux (Q_{LE}) imply an increase in humidity, while lower values of sensible heat flux (Q_H) imply lower atmospheric temperatures, both of which support the success of our mitigation strategy. However, it is important to acknowledge that, for the minimum energy point, the sensible heat flux transitions from having large negative values to high positive values (-175 W/m^2 to +335 W/m^2 at 4:00 PM), which is not desirable.

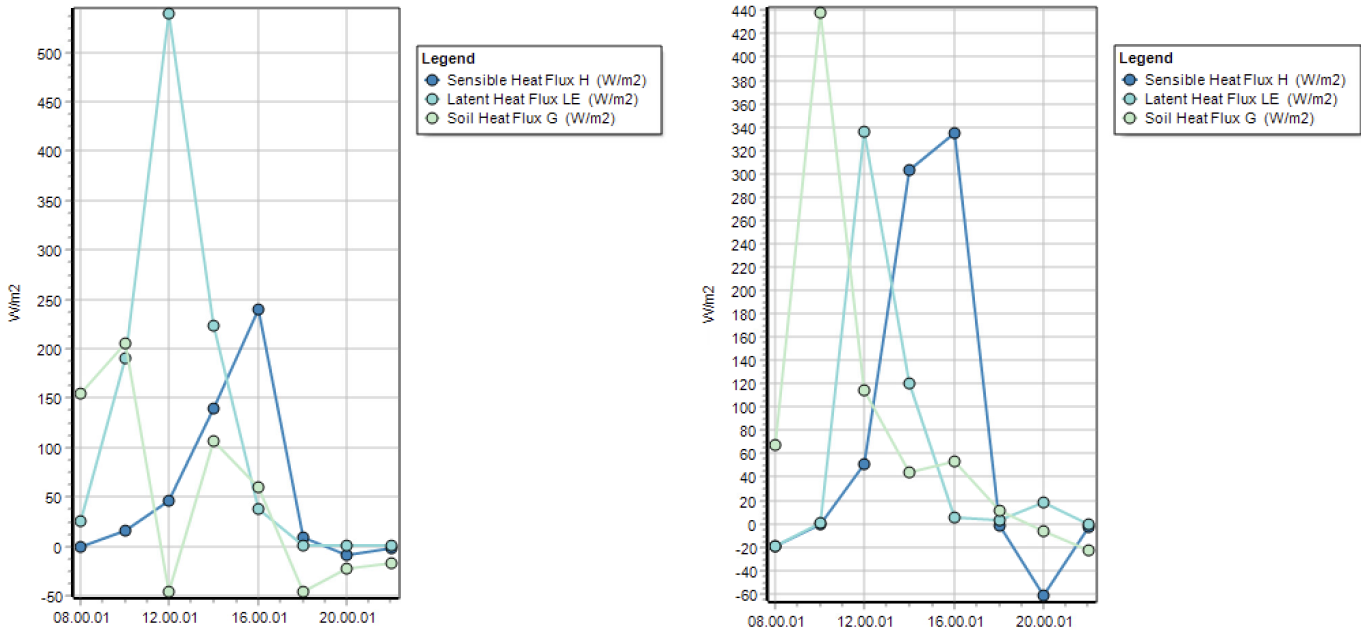

((a)) Maximal latent heat

((b)) Minimal latent heat

Figure 36: Energy balance for the building modification

8.3 Energy balance for the Ground modification

The latent heat flux shows its peak at 4:00 PM and a second peak at 12:00 PM whereas the soil heat flux is achieved at around 2:00 PM for the point with maximal latent heat. In contrast, the point with minimal latent heat shows a peak in latent heat later in the day, namely at around 18:00. In both figures (37(a) & 37(b)) the ground heat flux remains relatively low compared to the latent heat flux, indicating that the soil absorbs less heat, possibly due to vegetation cover or water reducing heat absorption. In the second graph (figure 39(b)), the latent heat flux (LE) is significantly lower compared to the first graph, which indicates less water availability or vegetation. In such a case, less evaporation takes place. The soil heat flux is positive from 8:00 AM to 7:00 PM indicating that the ground absorbs heat during this time period. After 7:00 PM it releases heat and thus shows negative values, peaking with -100 W/m^2 at 8:00 PM for poth points (Figure 37(b) and 37(a).

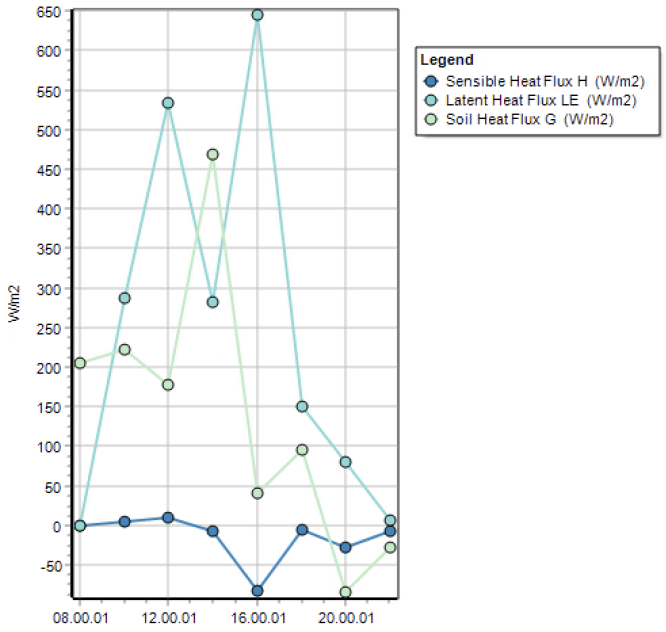

((a)) Maximal latent heat

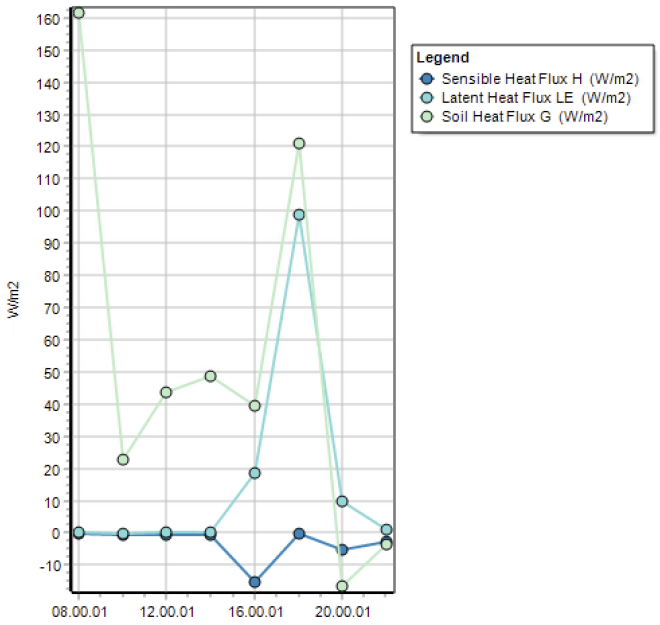

((b)) Minimal latent heat

Figure 37: Energy balance for the ground modification

8.4 Energy balance for the Water Body modification

The obtained results for the water body modification are shown in the following figure 38. It can be observed that the sensible heat fluctuates the most followed by the soil heat flux. The maximal latent heat flux with a value of around 590 W/m^2 takes place at noon which corresponds to the highest position of the sun and a minimal reflection angle of radiation. This peak indicates that a considerable amount of energy is used for evaporation. This could be explained by the location of the point at which the measurements were taken. The graph for the maximal latent heat (figure 38(a)) corresponds probably to the water body in between the buildings. The incoming radiation heats the water which then begins to evaporate. After 12:00 PM, the latent heat flux decreases rapidly but remains higher than the other fluxes until the late afternoon (4:00 PM). The sensible heat flux remains low for most of the morning but begins to rise around 12:00 PM, reaching a peak at 4:00 PM (+300 W/m^2). It can be observed in figure 38(a) that the soil heat flux is negative twice, which means that it releases energy in these time periods. One of the negative peaks is observed at noon, this could indicate that all the energy is used for evaporation as it takes place at the same time as the peak in latent heat flux. Figure 38(b) shows a significantly lower latent heat flux, its peak corresponds to +260 W/m^2 which is less than half of the maximum latent heat flux in figure 38(a).

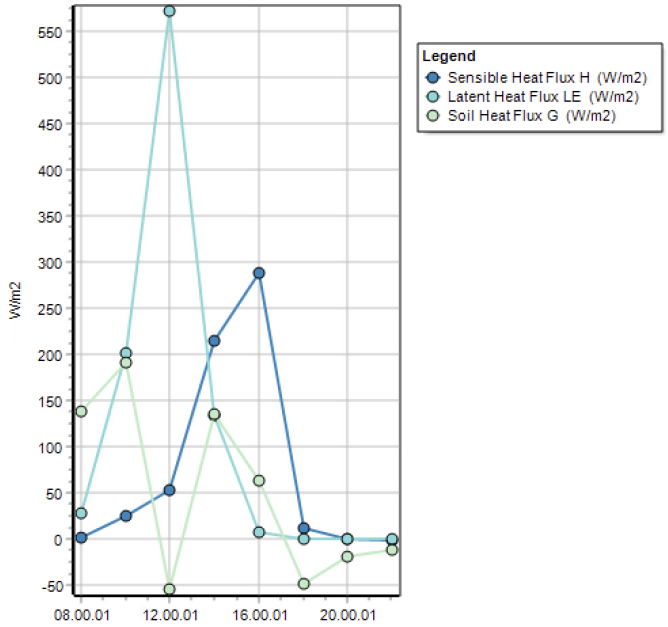

((a)) Maximal latent heat

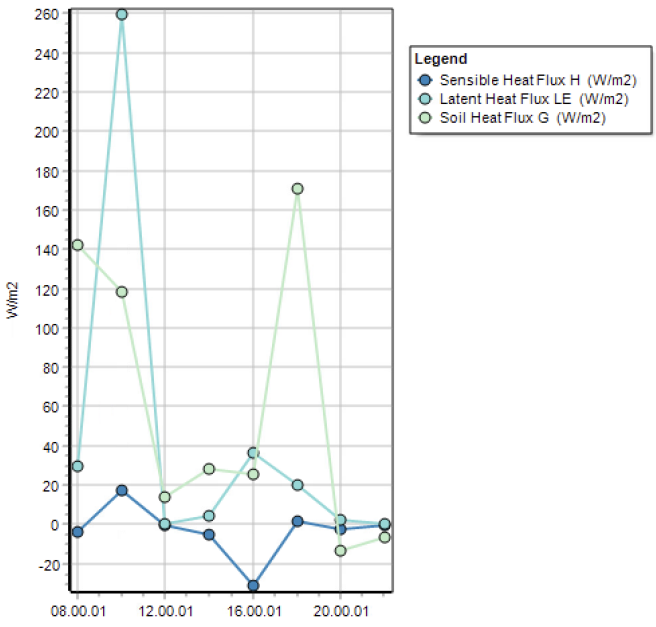

((b)) Minimal latent heat

Figure 38: Energy balance for water body modification

8.5 Energy balance for the Vegetation modification

As for the water bodies, the maximal latent heat can be observed at 12:00 PM whereas the minimal latent heat occurs 12:00 AM. But in comparison to figure38, the latent heat is in general lower. The vegetation still uses energy for evaporation but significantly less than water bodies. The sensible heat shows it peak for figure 39(a) at 4:00 PM whereas this is the negative peak for figure 39(b). It is remarkable that the curves of ground heat flux and latent heat flux in figure 39(b) are very similar. This could be due to the fact that both the ground heat flux and latent heat flux depend on surface energy availability. When incoming solar radiation heats the surface, part of the energy is transformed into ground heat flux. If there is no vegetation covering the ground, heat is well conducted into the soil.

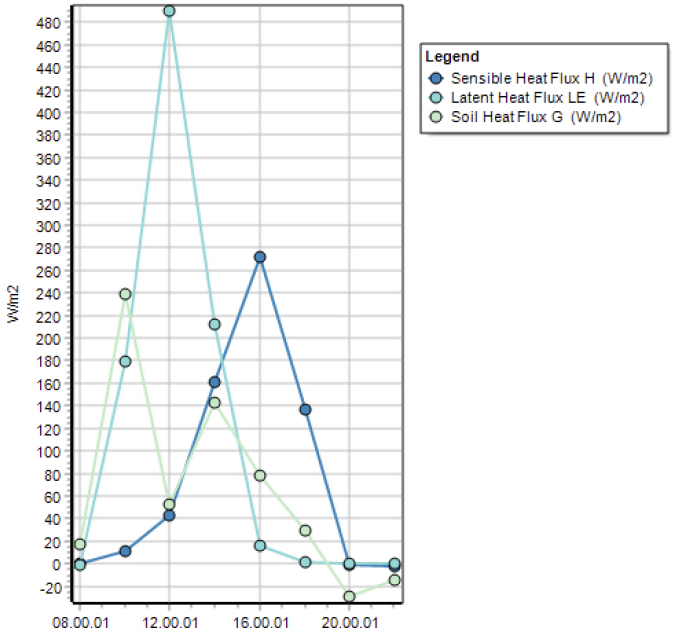

((a)) Maximal latent heat

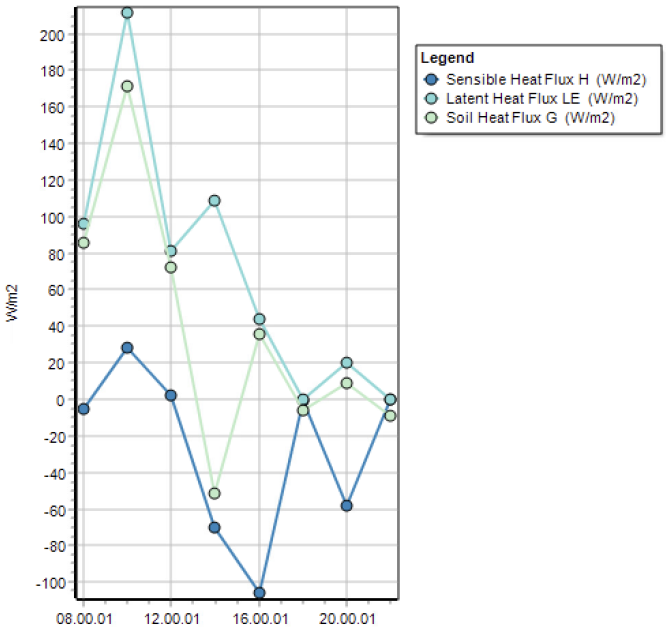

((b)) Minimal latent heat

Figure 39: Energy balance for the vegetation modification

9 Integrated Microclimate Solution

All the proposed solutions for each individuals cases are made in order to integrate them into one single mitigate solution which can be used to enhance microclimatic conditions in the EPFL Innovation Park. The goal isto optimize the differnets factors from air temperature to emission of radiation with a view to improve thermal comfort for users, in particular during summer time. As detailed before, every measure and idea have been taken so as to addressed key aspect of the base case scenario.

9.1 Potential air temperature

As we can see in the figure shown below, we have obtained significant improvements through the proposed mitigation measures. We observed an impressive reduction in air temperatures, particularly in zones near the buildings and green spaces. The most evident change is the global temperature reduction in the integrated solution. The addition of green roofs/facade vegetation, as well as the different openings, has permitted the enhancement of the cooling process thanks to the creation of shaded areas and the airflows that they offer (appearance of 35°C in the center of the site). The airflow created is very useful in the case of an urban environment because it offers a more comfortable space for users to work in. The replacement of the asphalt in the parking lot (thanks to the creation of an underground car park instead) with grass and trees has created a new cooler zone, which contrasts significantly with the base case where there was a very hot zone (around 38/37°C now as opposed to 41°C). Water bodies also contribute to this modification as they offer a new form of cooling through evaporation, creating a temperate microclimate. Overall, this solution shows a more uniform temperature distribution, which is very important for creating a more suitable working environment.

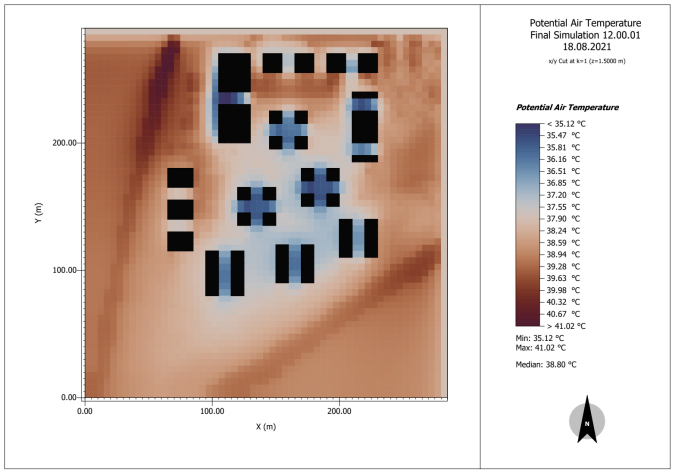

((a)) Integrated solution

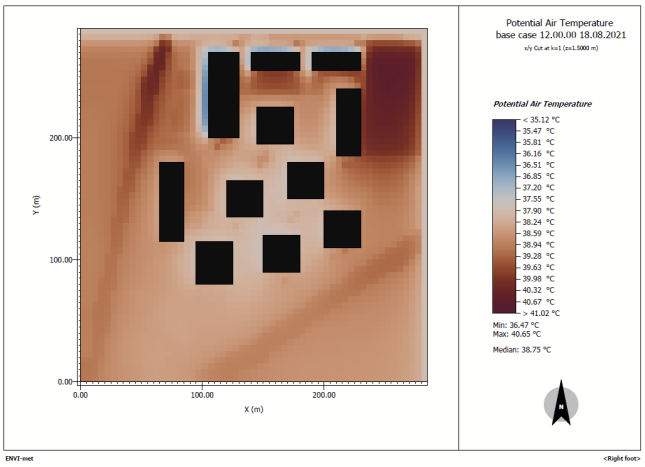

((b)) Base case

Figure 40: Potential air temperature diagram for the Integrated Solution

9.2 Relative humidity

Once again, the comparison between the integrated solution and the base case shows significant differences. As opposed to air temperature, there is now a global increase in relative humidity. Thankfully, this was the intended goal. In the integrated solution, higher relative humidity zones tend to appear near buildings, which are principally obtained due to the greening added to every building. These areas directly benefit from the vegetation, which tends to be more humid than plain concrete, thanks to the evapotranspiration it provides. Additionally, the water bodies increase the humidity levels that can be observed (it can go up to 66% compared to generally around 57% before). It can also be indicated that the former parking lot, which was particularly dry before, is now a new humid place that can be used to rest during the day, thus offering a new opportunity for a better quality of life. In general, the integrated solution effectively improves the relative humidity levels. There is now a more efficient and comfortable microclimate.

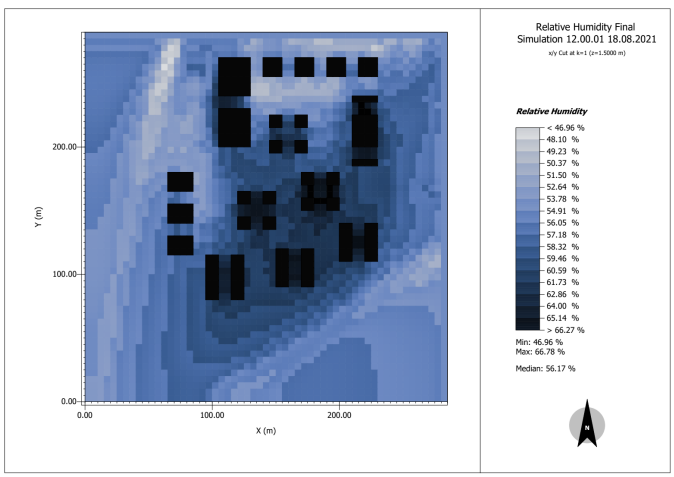

((a)) Integrated solution

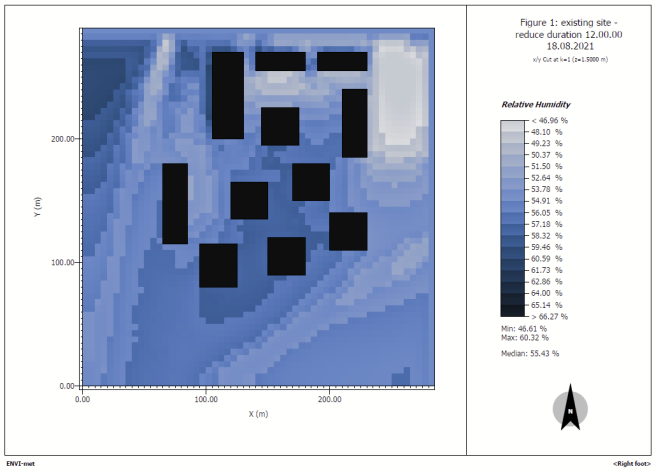

((b)) Comparison with base case

Figure 41: Relative humidity diagram for the Integrated Solution

9.3 Surface temperature

The comparison of surface temperatures between the two simulations shows major differences in temperature distribution across the site. The primary transformation, which is the parking lot, contributed significantly to temperature reduction through the introduction of grass and trees. These elements cool the surface and provide shading in the area.

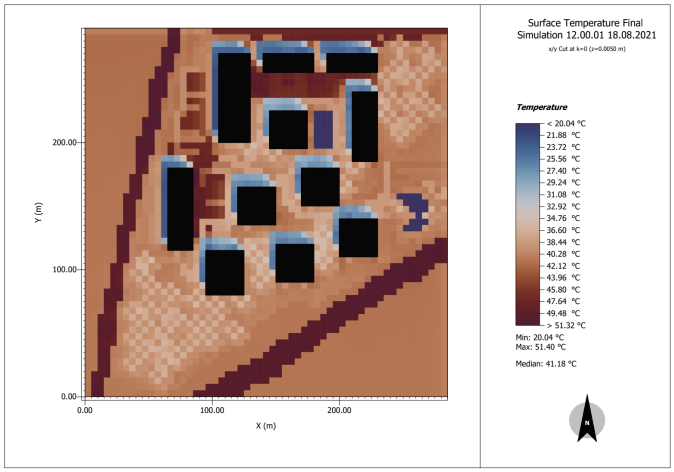

((a)) Integrated solution

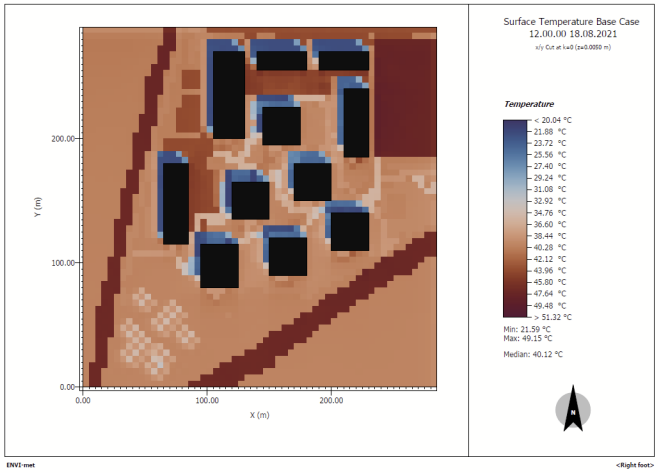

((b)) Base case

Figure 42: Surface temperature modification for the Integrated Solution

9.4 Wind

Unlike the others, the comparison in the wind speed diagrams revealed very little information that can be relevant for demonstrating the effectiveness of our design. The main reason for this is the lack of wind speed, even in the base case, which results in a similar situation in the integrated solution. Despite this, we can nevertheless emphasize the new pathways created in the integrated design. They show an increase in wind activity compared to the base case. The intention behind their creation was to channel airflow more effectively, particularly behind the north building, which previously acted as a wall for the air. The simulation revealed that these pathways work as intended, offering a new feeling of freshness on the site.

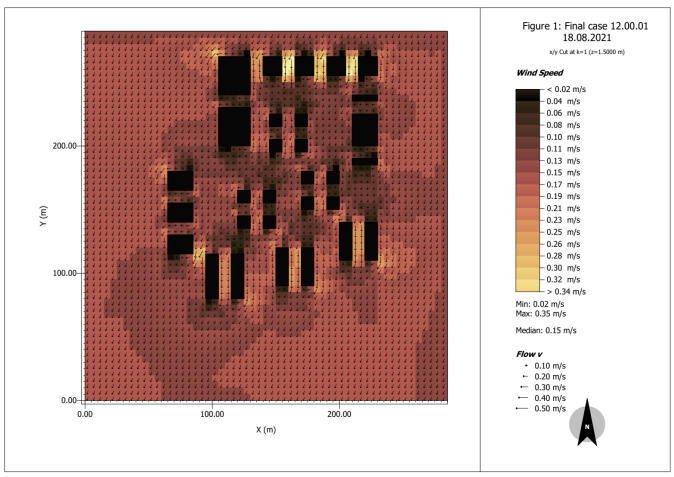

((a)) Integrated solution

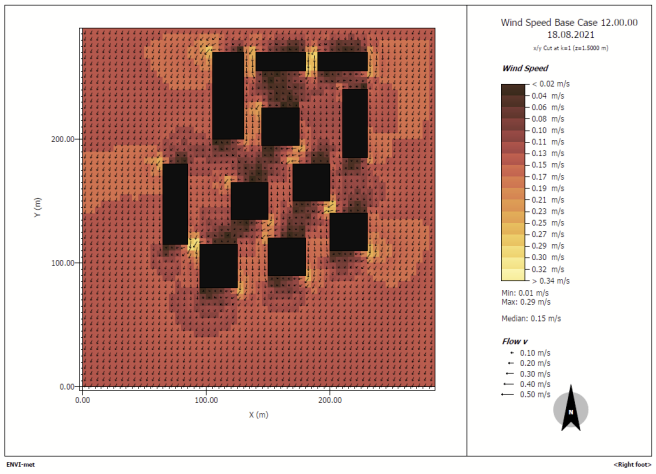

((b)) Base case

Figure 43: Wind diagram for the Integrated Solution

9.5 Radiation

Finally, the comparison between the radiation in the integrated simulation and the base one demonstrates significant differences across the site. It is clearly visible that there is a substantial decrease in reflection, with values not exceeding 250 W/m^2, compared to up to 400 W/m^2 in the base case scenario. One important measure that was implemented, and which shows promising positive results, is the replacement of materials with absorptive and impermeable surfaces by materials with lower absorption and greater permeability. This change reduces the formation of high-radiation areas, particularly along the pathways connecting the buildings. In general, the integrated solution achieves the intended goal and offers a more uniform radiation distribution across the site.

The reduced solar absorptance is likely leading to higher reflection of solar radiation, not lower as in your case. I think in this case, the reduction is due to less direct radiation reaching ground due to shading.

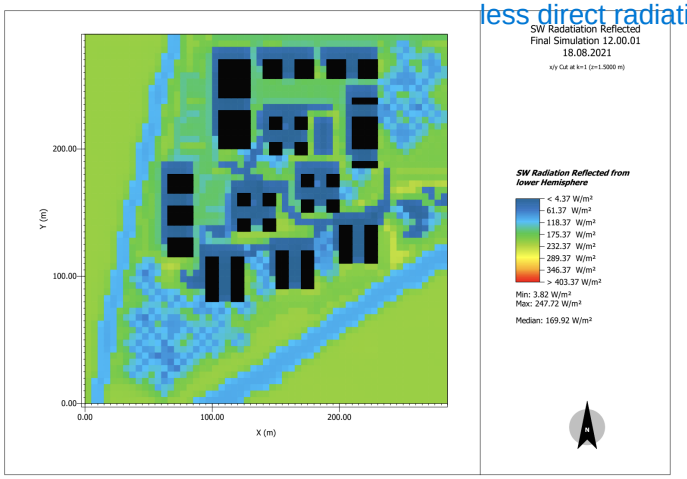

((a)) Integrated solution

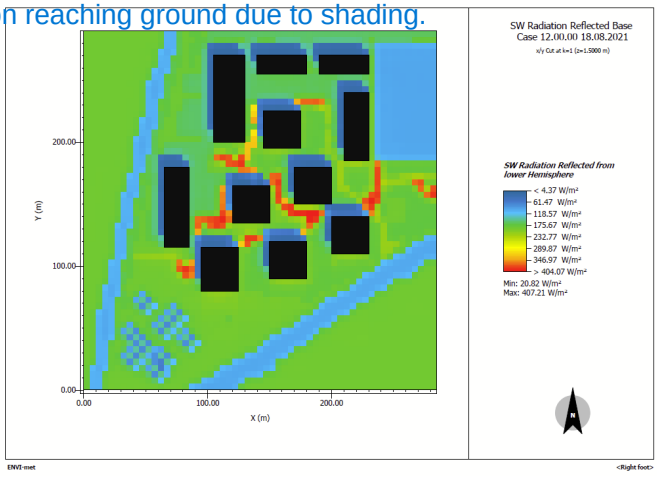

((b)) Base case

Figure 44: Radiation diagram for the Integrated Solution

9.6 Thermal Comfort

9.6.1 UTCI

There are notable variations in thermal comfort throughout the EPFL Innovation Park when comparing the Universal Thermal Climate Index (UTCI) graphs for the integrated solution with the base scenario. Improved thermal conditions and less heat stress for users across the site are reflected in the integrated solution's discernible decrease in UTCI values.
UTCI values are generally lower in the integrated solution, particularly in the vicinity of buildings, green

spaces, and bodies of water. The main reason for these benefits is the addition of vegetation, such as grass, trees, and green roofs, which offer shade, lessen heat absorption, and encourage cooling through evapotranspiration. On the other hand, because heat-retaining materials like concrete and asphalt predominate and exacerbate the Urban Heat Island effect, the base case shows greater UTCI values. By reducing surface temperatures, green areas added to the integrated solution—like the remodeled parking lot and walkways—significantly improve thermal comfort. In contrast to the default scenario, when the identical locations are marked by higher degrees of heat stress, these areas now function as cooler zones. Similarly, by using evaporative cooling, the integrated design's use of water bodies produces localized areas with less heat stress—an effect that isn't present in the base scenario.

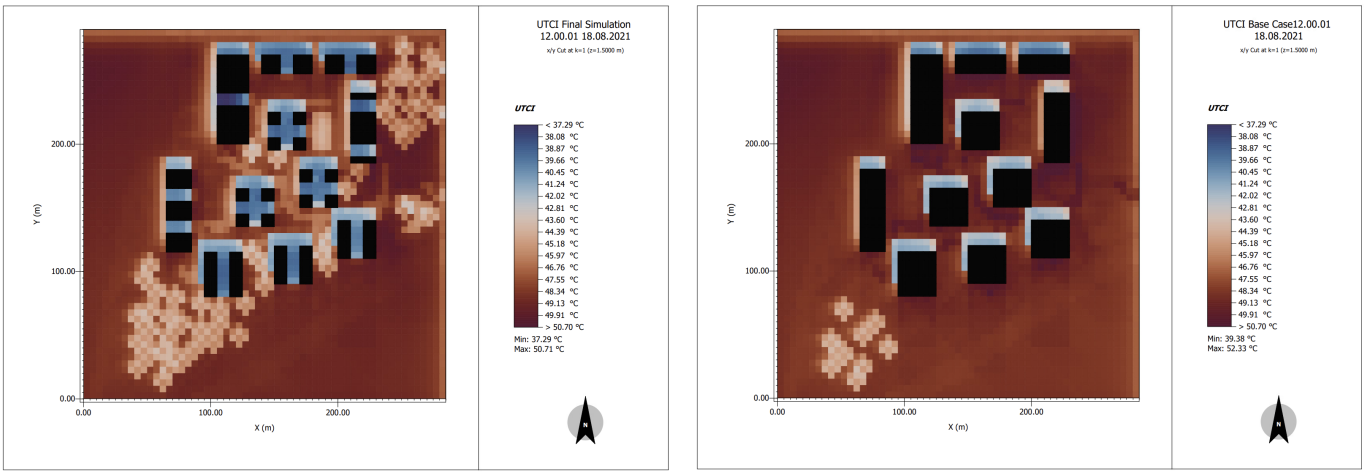

((a)) Integrated solution

((b)) Base case

Figure 45: UTCI diagram for the Integrated Solution

9.6.2 PET

The comparison between the Physiological Equivalent Temperature (PET) diagrams for the integrated solution and the base case highlights significant differences in thermal comfort across the EPFL Innovation Park. The integrated solution demonstrates a noticeable reduction in PET values, reflecting improved thermal conditions and a decrease in heat stress.

In the integrated solution, lower PET values are observed across the site, particularly near buildings, green spaces, and shaded zones. The main reduction are observed in the tunnels going through buildings, and seem to have a reducing impact on the direct surrounding environments. This improvement is attributed to the introduction of these tunnels, hidden from sun and radiation, and benefitting from rather cold material all around them (building material). The increase of vegetation, including green roofs, trees, and grass, reduces surface temperatures and enhance cooling through evapotranspiration and shading. In contrast, the base case exhibits higher PET values due to the predominance of heat-retaining materials such as asphalt and concrete, which exacerbate the Urban Heat Island (UHI) effect.

Open spaces, such as pathways and the transformed parking lot, also exhibit smaller improvements in thermal comfort in the integrated solution. These areas, now featuring grass and trees, provide shading and dissipate heat more effectively, resulting in lower PET values. In the base case, these same areas remain hotspots with higher PET values due to their impervious asphalt surfaces. Thermal comfort is also markedly improved in areas adjacent to buildings in the integrated solution. Green roofs, facade vegetation, and reflective building materials minimize the heat emitted from building surfaces, reducing PET values and improving comfort for users in these zones. Conversely, the absence of these measures in the base case leads to higher PET values around buildings, making these areas less comfortable. These areas are particularly important as they directly interact with the building. Entering and exiting the building lead to going in these areas, that become widely interacted with by humans. Thus, cooling these will have a great impact on how people will feel at the end of the day.

Overall, the integrated solution successfully mitigates heat stress and improves thermal comfort across the EPFL Innovation Park. Through strategic interventions, it achieves lower PET values and a more balanced microclimate, addressing the limitations of the base case and creating a more comfortable and sustainable urban environment. Once again, one might have expected bigger changes between the base case and the integrated solution. The extend of our changes is, again, a good path to explore, that could lead to greater variations.

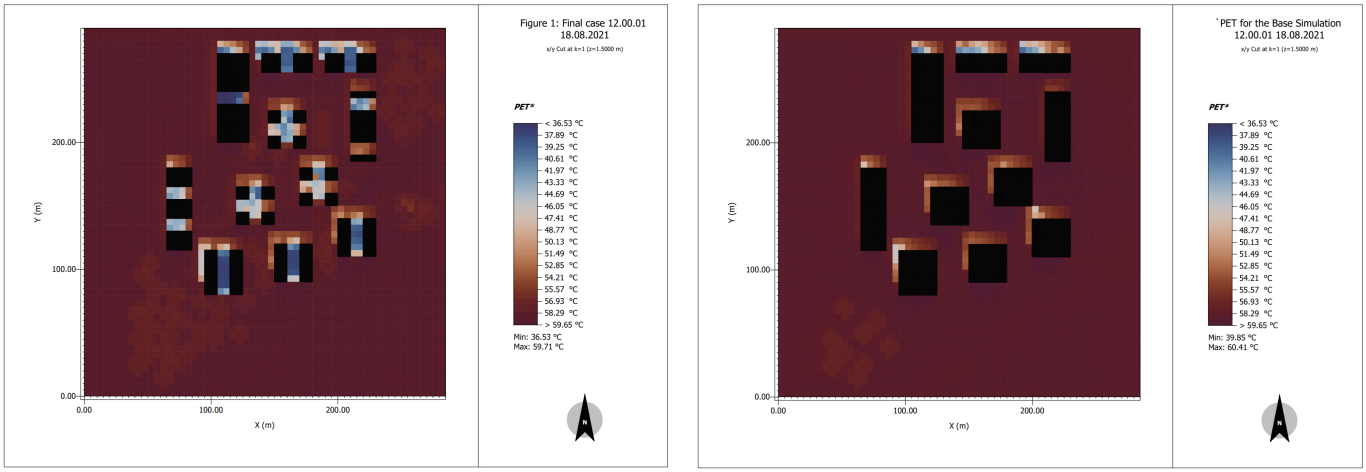

((a)) Integrated solution ((b)) Base case

Figure 46: PET diagram for the Integrated Solution

10 Conclusion

In summary, it can be said that different modifications lead to different results and that they influence each other. Overall, the combination of vegetation, water bodies and the tunnels in the buildings seem to be an effective mitigation solution as airflow is successfully increased and the UHI effect reduced. The integrated solution shows an improved microclimate with a focus on temperature reduction, increased humidity, lower radiation and increased comfort for users during summertime.

While the openings in the buildings have a local cooling effect, this modification does not appear to significantly influence the overall surface temperature. Most openings (those who align with the wind direction) increase air flow in the affected regions but the influence is not as big as we hoped for. But they provide shade for people that want to cross the campus. By modifying the floor, the surface temperature could be significantly reduced and evaporation was increased as the ground could as the soil can absorb and store more water.

The waterbodies contribute to cooling by evaporation and thermal inertia but the effect could be even stronger if their surface would be enlarged. However, they locally decreased significantly the surface temperature. Therefore, the two regularly shaped ponds in the simulation play a significant role in reducing the UHI effect, and the water body between the buildings contributes more efficiently to the cooling effect than the water body southeast of the buildings as it is located exactly where the UHI effect is greatest.

Vegetation, especially trees, plays a key role in reducing urban temperatures through shading, evapotranspiration, and carbon sequestration. The canopy coverage keeps the surface temperature lower and the influence on wind speed is relatively small so that the cooling effect provided by the wind is not excessively hindered. A sub-surface parking would lead to reduced surface temperature and therefore lower the UHI effect. It would also lead to less anthropogenic heat, even if this influence was neglected in the model. Instead of the previous parking lot, a green area could be placed, which would not only increase the thermal comfort of the users of the campus but would also contribute positively to the CO_2 balance. Therefore, vegetation, despite reducing wind speeds and consuming water that could otherwise evaporate, contributes to a reduced UHI effect and enhances human thermal comfort by providing shade and lowering radiation levels. One could attempt to further influence the UHI effect by installing green walls or rooftop gardens.

References

[1] Khovalyg, D. (2024). *CIVIL-309: Urban Thermodynamics* [Lecture slides]. EPFL.

[2] Oke, T. R., Mills, G., Christen, A., & Voogt, J. A. (2017). *Urban Climates*. Cambridge University Press. Retrieved from https://doi.org/10.1017/9781139016476

Building

[3] Bloomberg Originals. (2021). *Cómo Singapur utiliza la ciencia para mantenerse fresco* [YouTube video]. Retrieved from https://www.youtube.com/watch?v=PM101DvvG4Q

[4] Pignatta, G., & Ruefenacht, L. A. (2017). *Strategies for Cooling Singapore: A Catalogue of 80+ Measures to Mitigate Urban Heat Island and Improve Outdoor Thermal Comfort*. Cooling Singapore (CS). Retrieved from https://doi.org/10.3929/ethz-b-000258216

[5] Detomaso, M., Gagliano, A., Marletta, L., & Nocera, F. (2021). *Sustainable urban greening and cooling strategies for thermal comfort at pedestrian level*. Sustainability, 13(6), 3138. https://doi.org/10.3390/su13063138

Ground

[6] Sally Fakhri Khalaf Abdullah, and Tamarah Ameen Abdulkareem. “Urban Land Use Changes: Effect of Green Urban Spaces Transformation on Urban Heat Islands in Baghdad.” Alexandria engineering journal 66 (2023): 555–571. Web.

[7] ed. Innovation in Urban and Regional Planning: Proceedings of INPUT 2023 - Volume 1. 1st ed. 2024. Cham: Springer Nature Switzerland, 2024. Web.

Water bodies

[8] Le Phuc, Chi Lang, et al. “Cooling Island Effect of Urban Lakes in Hot Waves under Foehn and Climate Change.” *Theoretical and Applied Climatology*, vol. 149, no. 1–2, 2022, pp. 817–830. DOI: https://doi.org/10.1007/s00704-022-04085-6.

[9] Wang, Yasha, and Wanlu Ouyang. "Investigating the Heterogeneity of Water Cooling Effect for Cooler Cities." *Sustainable Cities and Society*, vol. 75, 2021, article 103281. DOI: https://doi.org/10.1016/j.scs.2021.103281.

[10] Syafii, Nedyomukti Imam, Masayuki Ichinose, Eiko Kumakura, Steve Kardinal Jusuf, Wong Nyuk Hien, Kohei Chigusa, and Yasunobu Ashie. “Assessment of the Water Pond Cooling Effect on Urban Microclimate: A Parametric Study with Numerical Modeling.” *International Journal of Technology*, vol. 12, no. 3, 2021, pp. 461–471. Web. DOI: https://doi.org/10.14716/ijtech.v12i3.4126.

[11] Saaroni, Hadas, and Baruch Ziv. "The Impact of a Small Lake on Heat Stress in a Mediterranean Urban Park: The Case of Tel Aviv, Israel." *International Journal of Biometeorology*, vol. 47, no. 3, 2003, pp. 156–165. DOI: https://doi.org/10.1007/s00484-003-0161-7.

Vegetation

[12] Gunawardena, K. R., et al. "Utilising Green and Bluespace to Mitigate Urban Heat Island Intensity." *The Science of the Total Environment*, vol. 584–585, 2017, pp. 1040–1055.DOI: https://doi.org/10.1016/j.scitotenv.2017.01.158.

[13] Shashua-Bar, Limor, et al. "The Influence of Trees and Grass on Outdoor Thermal Comfort in a Hot-arid Environment." *International Journal of Climatology*, vol. 31, no. 10, 2011, pp. 1498–1506. DOI: https://doi.org/10.1002/joc.2177

A Annex

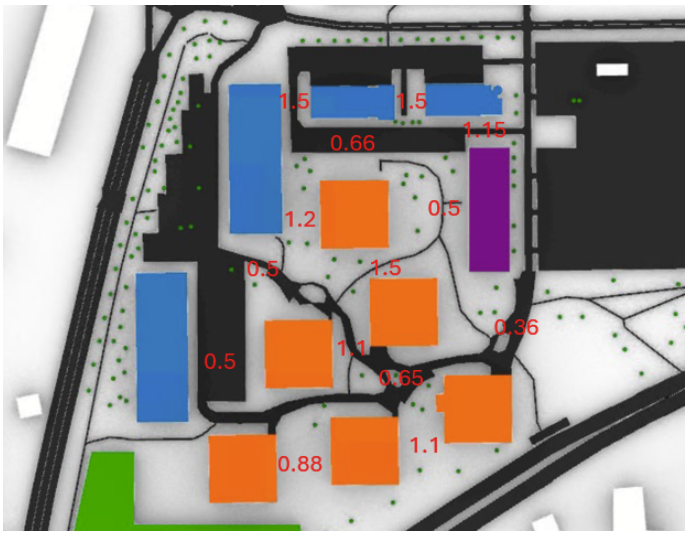

Figure 47: Canyon aspect ratios between the buildings

Category	Layer	Building Group A		Building Group B		Building Group C	
		Material	Thickness (m)	Material	Thickness (m)	Material	Thickness (m)
Façade	1	Prefabricated concrete wall	0.14	Plaster	0.01	Fiber cement board	0.008
	2	Insulation	0.1	EPS Expanded Polystyrene	0.18	Sandwich panel mineral wool	0.15
	3	Plaster	0.047	Plywood (heavyweight)	0.14	Aluminum	0.002
Roof	1	Gravel	0.05	Gravel	0.1	Gravel	0.04
	2	Insulation	0.2	XPS Extruded polystyrene CO2 blow	0.2	Mineral wool insulation	0.08
	3	Reinforced concrete slab	0.3	Concrete reinforced with 2% steel	0.3	Reinforced concrete slab	0.35
	4	--	--	EPS Expanded Polystyrene	0.065	--	--

Figure 48: Building materials for facade and roof

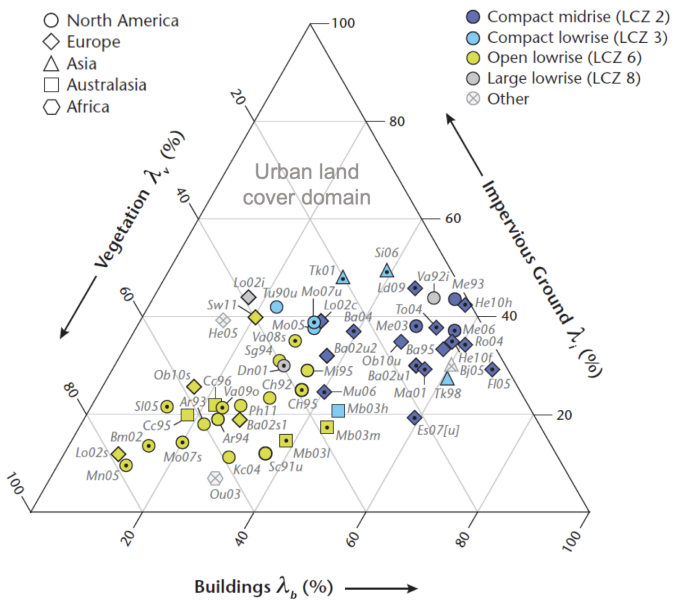

Figure 49: Important factors

Material	**Absorption (-)**	**Transmission (-)**	**Reflection (-)**	**Emissivity ϵ (-)**	**Specific Heat c (J/kg·K)**	**Thermal Conductivity λ (W/m·K)**	**Density ρ (kg/m^3)**
Prefabricated Concrete Wall	0.7	0	0.3	0.94	850	1.6	2200
Plaster	0.6	0	0.4	0.9	900	0.7	1400
Fiber Cement Board	0.5	0	0.5	0.9	900	0.19	1550
EPS Expanded Polystyrene	0.9	0	0.1	0.9	1.3	0.033	20
Sandwich Panel Mineral Wool	0.9	0	0.1	0.9	1200	0.042	195
Plywood (Heavyweight)	0.6	0	0.4	0.9	2200	0.16	600
Aluminum	0.2	0	0.8	0.9	880	160	2800
Gravel	0.8	0	0.2	0.9	1000	2	2200
XPS Extruded Polystyrene CO_2 Blow	0.9	0	0.1	0.9	1450	0.035	35
Mineral Wool Insulation	0.9	0	0.1	0.9	830	0.04	20
Reinforced Concrete (2%)	0.6	0	0.4	0.97	880	2.5	2400

Table 1: Thermal Properties of Building Materials

Figure 50: Aerial view of EPFL Innovation Park

Figure 51: Initial soil model of EPFL Innovation Park

A.1 Base case: Midnight analysis

A.1.1 Poential air temperature

At midnight the minimum and maximum temperatures drop to 32.62°C and 33.70°C, with the temperature range contracting from 4.18°C during the day to 1.08°C at night. This suggests that warmer zones lose more heat, leading to a more uniform thermal distribution.

Cooler areas are observed around buildings, forming a "redome" effect. Unexpectedly, the main road on the left and the parking lot on the right show lower temperatures, likely due to their exposed positions outside urban canyons, where nocturnal winds facilitate cooling.

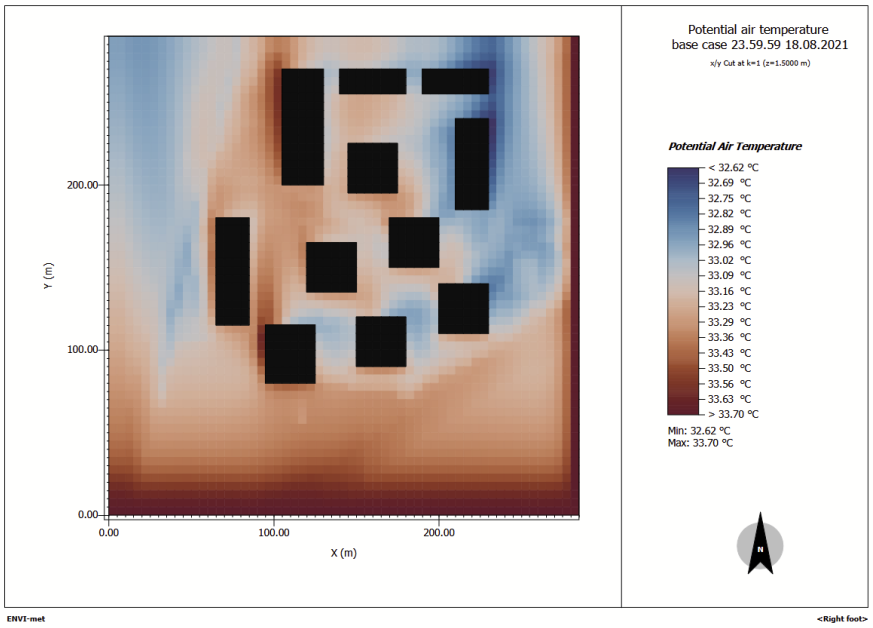

Figure 52: Potential air temperature diagram for the base case at midnight

A.1.2 Surface temperature

At midnight, the minimum surface temperature remains at 19.85°C, while the maximum decreases to 33.53°C, indicating a smaller temperature variation compared to daytime.

The zones behind the buildings show a slight temperature increase (∼2°C) as heat stored in the ground and building surfaces is gradually released, illustrating the thermal inertia of these materials. Asphalt and cement surfaces retain the highest temperatures due to their heat-retaining properties and low emissivity, with the warmest areas near Group A buildings. This is likely caused by heat release from prefabricated concrete facades, which exhibit high density, significant heat absorption, and moderate-to-low thermal conductivity.

In contrast, vegetated areas remain the coolest zones at night, as heat dissipates more rapidly due to the lower thermal inertia of vegetation and soil.

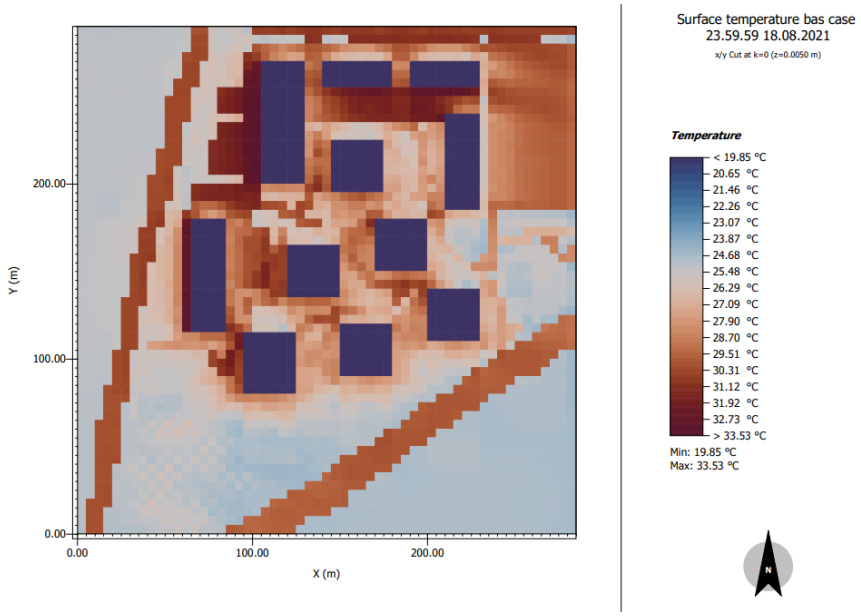

Figure 53: Surface temperature diagram for the base case at midnight

A.1.3 Wind patterns

At midnight (Figure 54 in Annex), the wind shifts to a south-to-north direction, with stronger activity compared to daytime as speed range increases to 0.03–1.10 m/s, enhancing nighttime airflow.

Stagnation zones form along the north and south building facades, while higher wind acceleration occurs at the corners. Wind corridors within urban canyons become more pronounced, improving localized airflow and ventilation in parts of the site.

Outside the building cluster, unobstructed wind flow at higher speeds facilitates air renewal, resulting in lower air temperatures in open zones like the parking lot and the road on the left. Conversely, lower wind speeds in the southern portion of the site impede heat dissipation, leading to localized warming (see Figure 52).

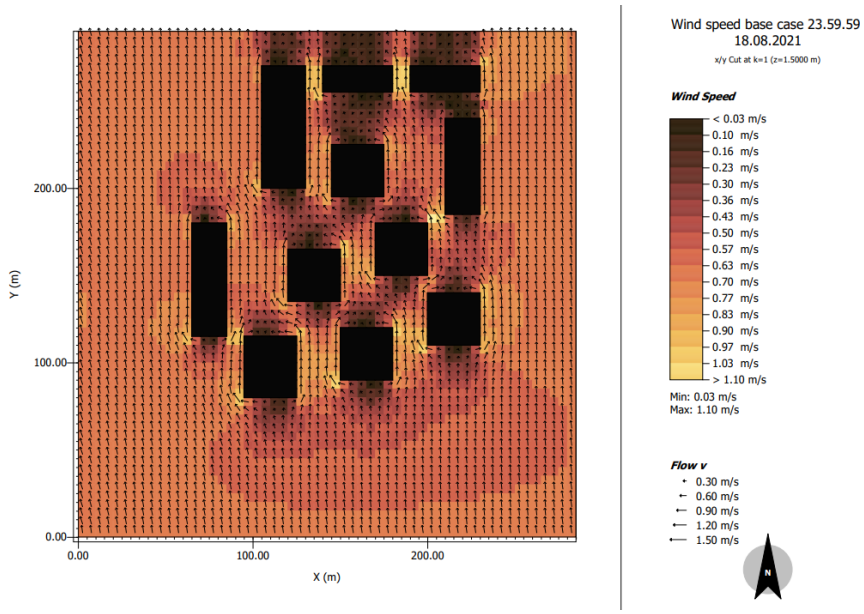

Figure 54: Wind diagram for the base case at midnight

A.1.4 Relative humidity

At midnight (Figure 55 in the Annex), the RH range increases to 64.57%–68.63%, driven by lower temperatures that reduce evaporation rates and moisture loss. Additionally, cooler temperatures mean the same absolute moisture content corresponds to higher RH values, further contributing to the increased range.

The more uniform nighttime distribution results from the absence of strong solar heating and temperature gradients, which limits localized moisture loss. Vegetation and shaded areas have less influence at night, as cooling no longer depends on shading or evapotranspiration. Similarly, the reduced impact of surface materials, as evidenced by the parking lot's high RH (66%), also contributes to this uniformity.

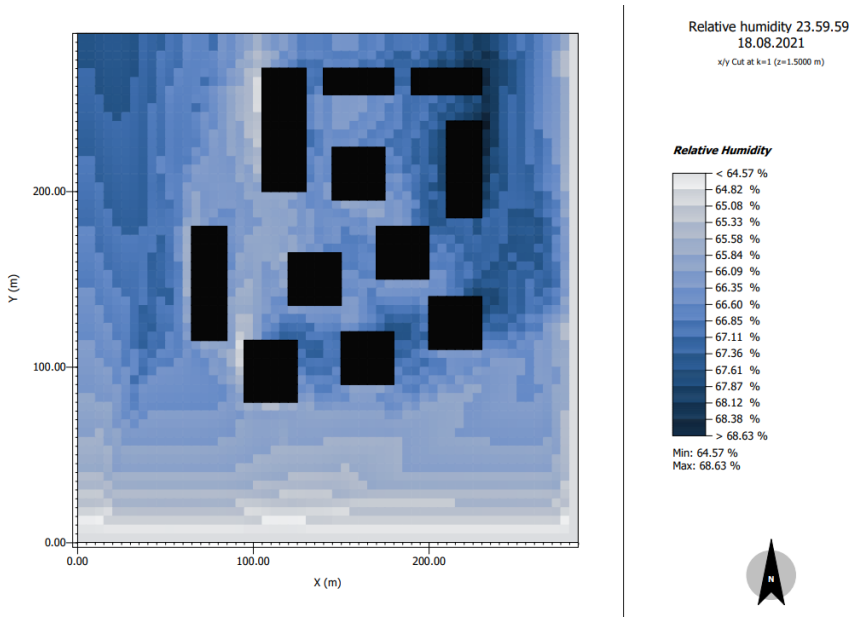

Figure 55: Relative humidity diagram for the base case at midnight

A.1.5 Radiation

As shortwave radiation is the predominate source of heat during daytime (solar radiation) while longwave radiation is the main source during nighttime, it is not possible to do a direct comparison for the parameter between the midday and midnight simulations results.

We must emphasize that, given the site's primary function as an office zone and our goal of improving the thermal environment for its occupants, the midnight analysis was conducted to gain a deeper understanding of the site's thermal behavior, particularly how heat dissipates overnight and influences subsequent daytime conditions. However, the midday simulation holds greater relevance for this report, as it better reflects the conditions experienced during active hours when people are present on-site and most susceptible to thermal discomfort. Consequently, the proposed mitigation solutions are evaluated based on the 12 pm simulation results only.

A.2 Building modifications

- **All Buildings:** Green roofs were installed across all structures to enhance thermal performance and mitigate urban heat island effects.
- **Building 1:** Ivy walls were added to the south and west facades. A centrally located opening hall (4 m high) was introduced on the south facade to improve airflow.
- **Building 2:** The building height was increased from 16 m to 18 m. Ivy walls were installed on the south and west facades, while the eastern facade featured a green wall (Fumbia up to 4 m, followed by ivy to the roof). A centrally located opening hall (4 m high) was added on the south facade.
- **Building 3:** The height was increased from 13 m to 18 m. Ivy walls were added to the south and west facades, and a centrally located opening hall (4 m high) was incorporated on the south facade.
- **Building 4:** The height was increased from 14 m to 16 m. Ivy walls were installed on the south and west facades, with two centrally located opening halls (each 4 m high) added to the south facade.
- **Buildings 5 and 8:** The height was reduced from 22 m to 16 m, and the material was changed from Material B to Material C. Ivy walls were added to the south facade, while the eastern facade featured a green wall (Fumbia up to 5 m, followed by ivy to the roof). Two centrally located opening halls (North-South and East-West, each 5 m high) were added to the south facade, along with a vertical central opening.
- **Building 6:** Ivy walls were placed on the south and west facades, with two centrally located opening halls (4 m high) added to the south facade.
- **Building 7:** Ivy walls were added to the south and west facades, while the eastern facade was fitted with a Fumbia wall up to 4 m. A centrally located, north-south opening hall (4 m high) was introduced on the south facade.
- **Building 9:** Similar modifications to Buildings 5 and 8, with ivy walls added to the south facade and a green wall (Fumbia up to 5 m, followed by ivy to the roof) on the eastern facade.
- **Building 10:** Ivy walls were installed on the south facade, while the eastern and western facades featured Fumbia walls up to 4 m. A centrally located, north-south opening hall (4 m high) was also added to the south facade.
- **Building 11:** Ivy walls were added to the south facade, while the eastern facade featured a green wall (Fumbia up to 4 m, followed by ivy to the roof). A centrally located, north-south opening hall (4 m high) was added to the south facade.